OAK RIDGE NATIONAL LABORATORY LIBRARIES

3 4456 0599463 5

CENTRAL RESEARCH LIBRARY

ORNL-4902
Vol. II

cy. 1

NEUTRON PHYSICS DIVISION

Annual Progress Report

Period Ending May 31, 1973

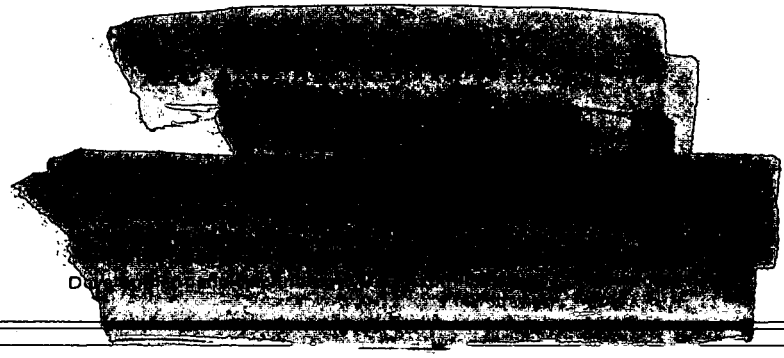

OAK RIDGE NATIONAL LABORATORY
CENTRAL RESEARCH LIBRARY
DOCUMENT COLLECTION
LIBRARY LOAN COPY
DO NOT TRANSFER TO ANOTHER PERSON
If you wish someone else to see this
document, send in name with document
and the library will arrange a loan.

UCN-7969
(3 3-67)

OAK RIDGE NATIONAL LABORATORY

OPERATED BY UNION CARBIDE CORPORATION • FOR THE U.S. ATOMIC ENERGY COMMISSION

Printed in the United States of America. Available from
the U.S. Atomic Energy Commission, Technical Information Center
P.O. Box 62, Oak Ridge, Tennessee 37830
Price: Printed Copy $5.40 ; Microfiche $0.95

[illegible] report of work sponsored by the United States Government. Neither the United States nor the United States Atomic Energy Commission, nor any of their employees, nor any of their contractors, subcontractors, or their employees, makes any warranty, express or implied, or assumes any legal liability or responsibility for the accuracy, completeness or usefulness of any information, apparatus, product or process disclosed, or represents that its use would not infringe privately owned rights.

ORNL-4902, Vol. II
UC-79d Liquid Metal Fast
Breeder Reactors Physics

Contract No. W-7405-eng-26

NEUTRON PHYSICS DIVISION
ANNUAL PROGRESS REPORT
For Period Ending May 31, 1973

F. C. Maienschein, Director

R. G. Alsmiller, Associate Director
C. E. Clifford, Associate Director
R. W. Peelle, Associate Director

AUGUST 1973

OAK RIDGE NATIONAL LABORATORY
Oak Ridge, Tennessee 37830
operated by
UNION CARBIDE CORPORATION
for the
U.S. ATOMIC ENERGY COMMISSION

ABBREVIATED CONTENTS

VOLUME I (UC-34c distribution — not included in this report)

INTRODUCTION

1. THEORETICAL STUDIES OF MEDIUM- AND HIGH-ENERGY RADIATION TRANSPORT
2. MEDIUM-ENERGY NUCLEON SPECTROSCOPY
3. WEAPONS RADIATION CROSS-SECTION STUDIES
4. WEAPONS RADIATION SHIELDING
5. RADIATION SHIELDING INFORMATION CENTER

PUBLICATIONS AND PAPERS PRESENTED AT SCIENTIFIC MEETINGS

VOLUME II (UC-79d distribution)

6. REACTOR CROSS-SECTION STUDIES
7. REACTOR CORE STUDIES
8. REACTOR SHIELDING

VOLUME II — CONTENTS

6. REACTOR CROSS SECTION STUDIES

6.0 Introduction -- R. W. Peelle ---------- 1

6.1 Tungsten Neutron Elastic- and Inelastic-Scattering Cross Sections from 4.34 to 8.56 MeV -- W. E. Kinney and F. G. Perey ---------- 2

6.2 ^{238}U Neutron Elastic-Scattering Cross Sections from 6.44 to 8.56 MeV -- W. E. Kinney and F. G. Perey ---------- 4

6.3 Measurement of the ^{238}U Capture Cross Section for Incident Neutron Energies up to 100 keV -- G. De Saussure, E. G. Silver, R. B. Perez, R. Ingle, and H. Weaver ---------- 4

6.4 Neutron Fission and Absorption Cross-Section Measurements for ^{239}Pu, ^{240}Pu, ^{241}Pu, and ^{241}Am -- L. W. Weston and J. H. Todd ---------- 4

6.5 Measurement of the Neutron Capture and Fission Cross Sections of ^{239}Pu and ^{235}U, 0.02 eV to 200 keV, the Neutron Capture Cross Sections of ^{197}Au, 10 to 50 keV, and Neutron Fission Cross Sections of ^{233}U, 5 to 200 keV -- R. Gwin, E. G. Silver, R. W. Ingle, and H. Weaver ---------- 6

6.6 Measurement of the Fission Cross Section of ^{235}U for Incident Neutron Energies Between 2 and 100 keV -- R. B. Perez, G. de Saussure, E. G. Silver, R. W. Ingle, and H. Weaver ---------- 8

6.7 Fission Neutron Multiplicity and Total Prompt Gamma-Ray Energy Following Fission in ^{239}Pu -- L. W. Weston and J. H. Todd ---------- 8

6.8 Multilevel Effects in the Unresolved Resonance Region -- G. de Saussure and R. B. Perez ---------- 9

6.9 The Transformation of a Set of Multilevel Resonance Parameters into an Equivalent Set of Single-Level Pseudoparameters and a "Smooth Background" -- G. De Saussure and R. B. Perez ---------- 12

6.10 Treatment of Large Perturbations of the Hamiltonian and the Boundary Conditions of a Quantum Mechanical System as an Initial Value Problem -- R. B. Perez and G. de Saussure - 12

6.11 The Optical Model -- G. R. Satchler and F. G. Perey ------ 13

6.12 Status Report on the Oak Ridge Electron Linear Accelerator (ORELA) - J. A. Harvey, T. A. Lewis, F. C. Maienschein, and H. A. Todd ---------- 14

7. REACTOR CORE STUDIES

7.0 Introduction -- F. R. Mynatt ---------- 18

7.1 TASK - A Generalized One-Dimensional Transport and Diffusion and Kinetics Code -- A. R. Buhl, H. L. Dodds, Jr., J. C. Robinson, and R. A. Lillie ---------- 19

7.2 Intercomparison of Nonperturbing Techniques for Inferring the Reactivity of Fast Reactors -- A. R. Buhl, J. C. Robinson, and E. T. Tomlinson ---------- 20

7.3 One-Dimensional Calculations in Support of the Reactivity Surveillance Procedures for the Fast Test Reactor -- G. F. Flanagan, D. B. Simpson, and A. R. Buhl ---------- 21

7.4 Calculated Kinetics Parameters for the Southwestern Experimental Fast Oxide Reactor Assemblies I-P, II-A, and II-C -- W. A. Rhoades ---------- 21

7.5 Verification of a New Method for Calculating and Measuring Generation Time in a Subcritical Fast Reactor -- A. R. Buhl and J. C. Robinson ---------- 22

7.6 The Status of Subcritical Reactivity Determination for LMFBRS -- A. R. Buhl, N. J. Ackermann, Jr., and J. C. Robinson ---------- 22

8. REACTOR SHIELDING

8.0 Introduction -- C. E. Clifford and F. R. Mynatt ---------- 26

8.1 Fast Reactor Experimental and Analytical Shielding Monthly Progress Reports, June and July, 1972, 189a No. 10028, Activity No. 40 01 61 -- F. R. Mynatt et al. ---------- 30

8.2 Fast Reactor Experimental Shielding Monthly Progress Reports August, 1972 - March, 1973, 189a No. 10028, Activity No. 40 01 03 1 -- F. R. Mynatt et al. ---------- 31

8.3 Fast Reactor Analytical Shielding Monthly Progress Reports, August, 1972 - February, 1973, 189a No. 10318, Activity No. 40 01 03 -- F. R. Mynatt et al. ---------- 33

8.4 SDT1-SDT5: Broomstick Experiments to Check Neutron Total Cross Sections for Iron, Oxygen, Nitrogen, Sodium, and Stainless Steel -- R. E. Maerker ---------- 35

8.5 SDT6-SDT7: Experiments on Secondary Gamma-Ray Production in Iron, Stainless Steel, Oxygen, Nitrogen, and Sodium -- R. E. Maerker ---------- 35

8.6 The Absolute Neutron Spectrum Emerging Through a 15-1/4-in. Collimator from the TSR-II Reactor at the Tower Shielding Facility -- R. E. Maerker and F. J. Muckenthaler ---------- 36

8.7 The ORNL Benchmark Experiment for Neutron Transport in Iron and Stainless Steel -- R. E. Maerker and F. J. Muckenthaler ---------- 36

8.8 The ORNL Benchmark Experiment for Neutron Transport in Thick Sodium -- R. E. Maerker, F. J. Muckenthaler, and C. E. Clifford ---------- 37

8.9 ORNL TSF Pipe Chase Neutron Streaming Experiment - Phase One -- B. J. McGregor, F. R. Mynatt, F. J. Muckenthaler, and C. E. Clifford ---------- 37

8.10 FFTF Pipe Chase Streaming Experiment - Phase Two -- B. J. McGregor and F. J. Muckenthaler ---------- 38

8.11 LMFBR Radiation Transport Methods Development -- F. R. Mynatt, M. L. Gritzner, L. R. Williams, and C. E. Clifford -- 41

8.12 Neutron Cross-Section Sensitivity Analysis: A General Approach Illustrated for a Na-Fe System -- D. E. Bartine, E. Oblow, and F. R. Mynatt ---------- 42

8.13 The Development and Application of a Discrete Ordinates Adjoint Difference Method for One-Dimensional Shield Weight Optimization -- R. L. Childs, W. W. Engle, Jr., J. C. Robinson, and F. R. Mynatt ---------- 42

8.14 A Perturbation Method for Shield Weight Optimization -- R. L. Childs, J. C. Robinson, W. W. Engle, Jr., and F. R. Mynatt ---------- 43

SECTION 6. REACTOR CROSS SECTION STUDIES

6.0 INTRODUCTION

R. W. Peelle

The cross section studies described in this section were performed to support the fast breeder reactor program, though many of the measurements have broader application. The prime emphasis has been on neutron capture and fission cross sections of the fertile and fissile nuclides known to have a dominant effect on the performance of the core-blanket portion of the breeder.

The first two papers (6.1 and 6.2) consist of abstracts of final reports on experimental work performed some time ago at the Van de Graaff facility on neutron scattering in the 4- to 9-MeV range of incident energies. Within a few months the remainder of these reports, covering N, Cr, Ni, Ti, ^{54}Fe, ^{63}Cu, ^{65}Cu, ^{207}Pb, and ^{208}Pb will join the ones mentioned here on W and ^{238}U. These data are of great interest in shield design and form a reasonably large fraction of the world's data base for scattering of neutrons in this energy region. Thus they will for some time retain an important role in the generation of evaluated data files for neutron scattering. The results for medium-weight nuclides have shown that an "evaporation" energy distribution is only a modestly good approximation to the overlapping structure seen in the spectra for excitation energies above those corresponding to the well-separated levels near the ground state. A few states or groups of states receive the bulk of the overall intensity. Current work in neutron elastic and inelastic scattering is centered at the Oak Ridge Electron Linear Accelerator (ORELA) where the year has been spent in setting up equipment to be used for neutron elastic and inelastic scattering studies. The inelastic scattering cross sections will be measured by observing the deexcitation gamma rays.

In studies of capture and fission cross sections of fertile and fissile nuclides, our group accepts serious roles in acquisition and interpretation and in aiding evaluation. Emphasis has been placed on the cross sections shown by past sensitivity analyses to be of dominant importance. The capture and fission cross sections in the upcoming fourth version of the official evaluated nuclear data file (ENDF/B-IV) is to be based predominantly on the new measurements of our group at ORELA for energies below 100 keV for ^{235}U, ^{239}Pu, ^{240}Pu, and ^{241}Pu, and the file for capture in ^{238}U will be very strongly influenced by our work (see papers 6.3 - 6.6). In the case of the work reported on ^{240}Pu and ^{241}Pu, required accuracies are expected to be met by the work now underway for the energy region studied. For capture measurements in ^{239}Pu and ^{235}U, we will await reevaluation of the need before attempting more precise measurements, but for fission measurements in ^{235}U and ^{239}Pu and for capture measurements in ^{238}U, one or more "rounds" of very serious improvement of experiment and analysis technique appear to be required to permit sufficiently precise reactor design. Experimental work is also required on the absolute fission neutron multiplicity of ^{239}Pu as a function of incident energy, so we are now undertaking an experiment in this area.

In the area of cross-section interpretation and evaluation, there has been a question for a long time whether or not the single-level resonance formulation adequately represents the cross sections of the fissile nuclides for fast reactor calculations particularly in the unresolved resonance region. For these nuclides both theory and precise fitting of point cross sections in the resonance region do require a multilevel treatment. Paper 6.8 deals with this question and concludes that for ^{235}U at the operating temperature of a fast reactor, the multilevel formulation is not required in the unresolved resonance region. The multilevel formulation may be needed in the resolved region to obtain the average total resonance width for use in extrapolating to the unresolved region.

Cross-section evaluation work is not explicitly reported here. Experimenters did make considerable efforts to transmit data and writeups in appropriate forms to the evaluators working on ENDF/B-IV. Important testing work on evaluated data files was performed within the Radiation Shielding Information Center, and the evaluation group under AEC-DRDT sponsorship worked on complete ENDF/B-IV evaluations for carbon and sodium and a partial evaluation for iron. The file just prepared for carbon is particularly significant because it is the first to contain uncertainty quantities within the formatted file. The whole system being used for handling uncertainty quantities within the official evaluated files was developed in our group this year to meet the first-order needs for determination of the uncertainties in calculated reactor parameters and for cross-section sensitivity analyses.

The last paper in the section (6.12) summarizes activities at the linear accelerator itself. Considerable progress was made toward improved performance and reliability of the facility.

6.1 TUNGSTEN NEUTRON ELASTIC- AND INELASTIC-SCATTERING CROSS SECTIONS FROM 4.34 TO 8.56 MeV[1]

W. E. Kinney and F. G. Perey

Measured natural tungsten neutron elastic- and inelastic-scattering cross sections are presented and shown to be in good agreement with the results of others. An evaporation model of inelastic scattering was found to be applicable with nuclear temperatures in agreement with previous results but with total inelastic cross sections larger by as much as 20% than measured nonelastic cross sections. ENDF/B W (Mat 1060-63) elastic angular distributions agree with our data at angles less than 50 deg but do not agree at larger angles. The ENDF/B nuclear temperatures are 10-15% lower than experimental temperatures. (Typical data are compared with the results of others in Fig. 6.1.1.)

[1]Abstract of ORNL-4803 (May 1973).

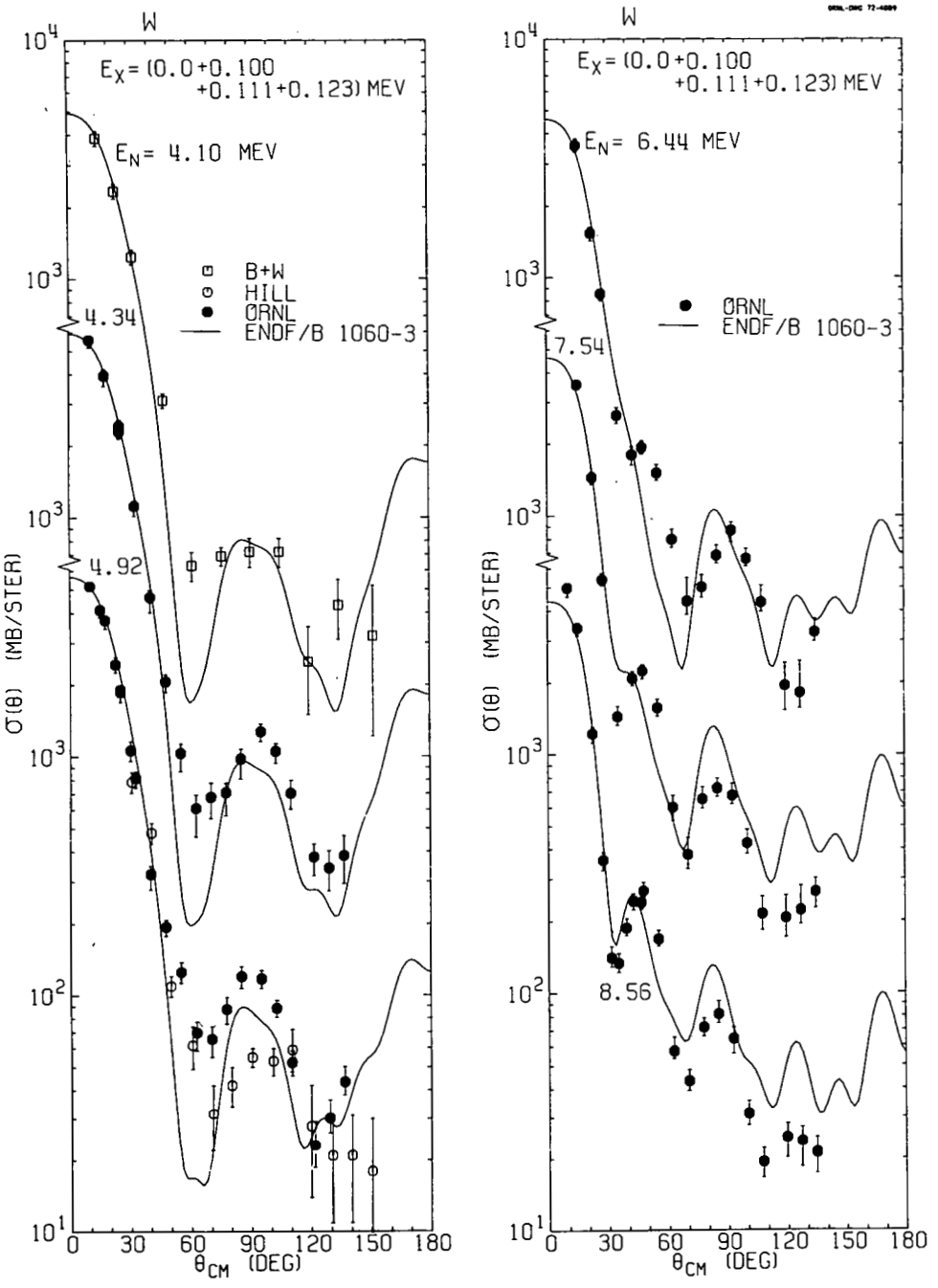

Fig. 6.1.1. Our Neutron Differential Cross Sections for Natural Tungsten for Elastic Scattering and Inelastic Scattering to Levels ≤ 0.123 MeV Together with the Data of Beyster and Walk (B&W) and Hill. The curves are ENDF/B elastic differential cross sections for the tungstel isotopes (Mat 1060 through Mat 1063) combined with natural isotopic abundances and normalized to the experimental integrals.

6.2 ^{238}U NEUTRON ELASTIC-SCATTERING CROSS SECTIONS FROM 6.44 TO 8.56 MeV[1]

W. E. Kinney and F. G. Perey

Measured ^{238}U neutron differential cross sections for elastic scattering (plus inelastic scattering to levels $\leq$ 0.309 MeV) at incident neutron energies of 6.44, 7.54, and 8.56 MeV are presented. The data are in agreement with previous results. ENDF/B MAT 1158 elastic angular distributions are in excellent agreement with experimental results from 6.4 to 8.56 MeV. The ENDF/B 1158 angle-integrated elastic cross section represents a reasonable fit to experimental results from 4 to 8.5 MeV.

[1]Abstract of ORNL-4804 (June 1973).

6.3 MEASUREMENT OF THE ^{238}U CAPTURE CROSS SECTION FOR INCIDENT NEUTRON ENERGIES UP TO 100 keV[1]

G. de Saussure, E. G. Silver, R. B. Perez,
R. Ingle[2] and H. Weaver

The neutron capture cross section of ^{238}U was measured for incident neutron energies between 5 eV and 100 keV using a pulsed electron linac neutron source and the time-of-flight technique. Capture gamma rays were detected by a large liquid scintillator located on a 40-m flight path. The incident neutron flux was monitored by a $^{10}BF_3$ ionization chamber. The cross section was normalized by the saturated resonance technique. This memorandum contains a brief description of the experimental technique and a discussion of the results. A complete tabulation of one of the measurements is given in the appendix. (Typical data are compared with the results of others in Fig. 6.3.1.)

[1]Abstract of ORNL-TM-4059 (February 1973).
[2]Instrumentation and Controls Division.

6.4 NEUTRON FISSION AND ABSORPTION CROSS-SECTION MEASUREMENTS FOR ^{239}Pu, ^{240}Pu, ^{241}Pu AND ^{241}Am[1]

L. W. Weston and J. H. Todd[2]

The neutron fission and absorption cross sections for ^{239}Pu, ^{240}Pu, and ^{241}Pu were measured from thermal-neutron energies up to 20 keV. In addition, the absorption cross sections of ^{240}Pu and ^{241}Am were measured from thermal-neutron energies to 200 keV. The ratio of the capture and fission cross sections, $(\sigma_c)/(\sigma_f)$, could be determined up to 200 keV for ^{239}Pu and ^{241}Pu.

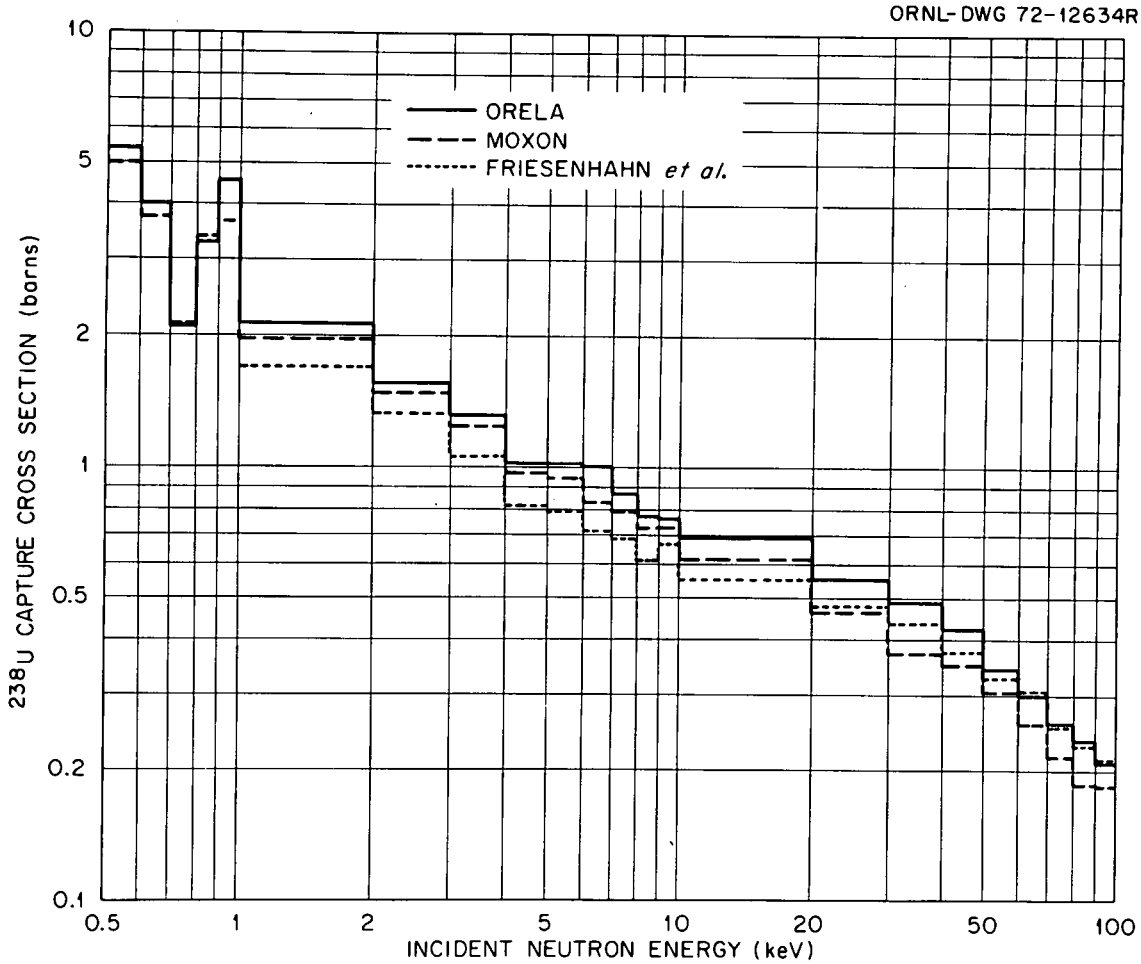

Fig. 6.3.1. A Comparison of the Average $^{238}U(n,\gamma)$ Cross Sections Obtained by de Saussure and Perez with Those of Some Other Authors. Since this cross section should be known to a few percent for FBR design, the 15% differences represent a considerable problem. Significant efforts have already been made by the authors to determine the source of the discrepancies. Note that the actual cross section in these regions is by no means smooth; nearly isolated resonances are visible in the data at energies as high as a few keV.

The general trends of the ^{239}Pu and ^{241}Pu data have been reported previously.[3] The average absorption cross section of ^{240}Pu is in agreement with that reported by Hockenbury.[4] The shape of the two sets of data is in good agreement over the range of overlap. The present data, which are normalized to the thermal cross section, are about 10% lower than that of Hockenbury at keV neutron energies. Both these normalizations are appreciably higher than ENDF III; however, all of the data on which ENDF-III was based have been renormalized upward. The average absorption cross section for ^{241}Am was in good agreement with ENDF-III up to 20 keV and is appreciably higher thereafter. There were little previous data on ^{241}Am available in the energy range from 20 to 200 keV.

These results, although not complete, have been reported to the ENDF-IV committee and will be considered in the revision of the ENDF data. (Typical data are shown in Fig. 6.4.1.)

[1]Reprint of Paper 25 in "Report to the U. S. Nuclear Data Committee," compiled by F. G. Perey (April 1973).

[2]Instrumentation and Controls Division.

[3]L. W. Weston and J. H. Todd, Trans. Am. Nucl. Soc. 15, 480 (1972).

[4]R. W. Hockenbury, W. R. Moyer, and R. C. Block, Nucl. Sci. Eng. 49, 153-161 (1972).

6.5 MEASUREMENT OF THE NEUTRON CAPTURE AND FISSION CROSS SECTIONS OF ^{239}Pu AND ^{235}U, 0.02 eV TO 200 keV, THE NEUTRON CAPTURE CROSS SECTIONS OF ^{197}Au, 10 TO 50 keV, AND NEUTRON FISSION CROSS SECTIONS OF ^{233}U, 5 TO 200 keV[1]

R. Gwin, E. G. Silver, R. W. Ingle,[2] and H. Weaver

The neutron capture and fission cross sections for ^{239}Pu and ^{235}U have been measured over the neutron energy region from 0.02 eV to 200 keV and the fission cross section for ^{233}U has been measured from 5 to 200 keV. The fissile isotopes were contained in multiplate ionization chambers. The ^{197}Au neutron capture cross section has been measured from 10 to 50 keV. A detailed comparison of the present data has been made with other experimental data and with the ENDF/B-III evaluation.

[1]Abstract of paper prepared for submission to Nuclear Science and Engineering.

[2]Instrumentation and Controls Division.

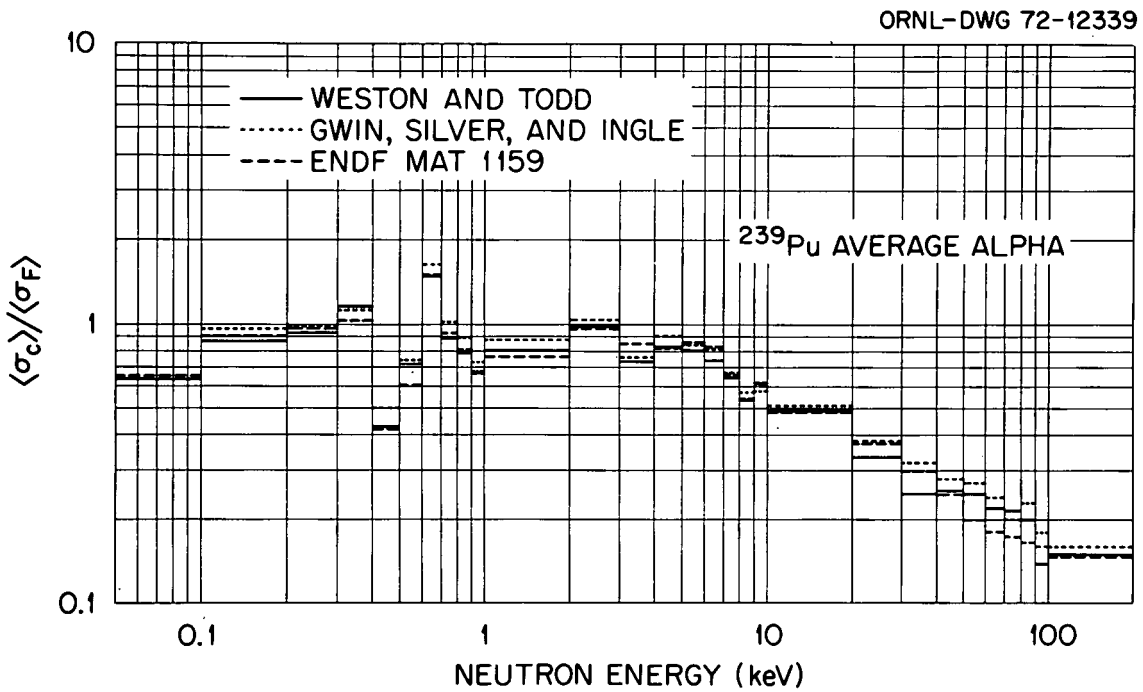

Fig. 6.4.1. A Comparison of the Ratio of Average Capture to Fission Cross Sections for ^{239}Pu as Determined in Preliminary Results from Independent ORELA Experiments of Weston and Todd and of Gwin, Silver, and Ingle. Values from ENDF/B-III are also shown. Four years ago similar comparisons of available data showed discrepancies of as much as a factor of two.

6.6 MEASUREMENT OF THE FISSION CROSS SECTION OF ^{235}U FOR INCIDENT NEUTRON ENERGIES BETWEEN 2 AND 100 keV[1]

R. B. Perez, G. de Saussure, E. G. Silver,
R. W. Ingle,[2] and H. Weaver

The fission cross section of ^{235}U was measured for incident neutron energies between 2 and 100 keV using an electron Linac pulsed source of neutrons and the time-of-flight technique. The fission events were characterized by coincidence between the pulses of a fission chamber, placed at the center of a large scintillation tank, and gamma-ray events registered in the tank. The incident neutron flux vs energy was monitored by a BF_3 ionization chamber and checked with a ^6Li-glass neutron detector. The cross sections were normalized to a value of 31643 barns x eV for the fission integral between 2 and 10 keV.

The comparison of the present ^{235}U fission cross-section results with the values from other sources show that in the energy region covered by this experiment there is in general an agreement within 3 to 5%.

The previously reported intermediate structure in the fission cross section in the keV region is confirmed by the results of this work.

[1]Abstract of paper prepared for submission to Nuclear Science and Engineering.
[2]Instrumentation and Controls Division.

6.7 FISSION NEUTRON MULTIPLICITY AND TOTAL PROMPT GAMMA-RAY ENERGY FOLLOWING FISSION IN ^{239}Pu[1]

L. W. Weston and J. H. Todd[2]

There have been several contradictions[3-5] concerning the fission neutron multiplicity for ^{239}Pu. These experiments were concerned with the resonance region of neutron energies below about 200 eV. At one time there was reported a rather strong correlation of the fission neutron multiplicity with resonance spin. After additional experiments by the authors and by others[6,7] there appears to be no strong, direct correlation with neutron spin. There remain variations with neutron energy and variations from resonance to resonance which are statistically significant. In our previous data[5] there was a small ($\sim$ 1.5%) oscillation of the values of $\bar{\nu}$ with neutron energy. These variations are not surprising in a physical process as complicated as fission.

Recently there has been an experiment[7] which indicates an appreciably wider variation of $\bar{\nu}$ from resonance to resonance but still not directly correlated with spin. The theoretical explanation proposed by Shackelton et al.[7] is that $\bar{\nu}$ is correlated with the fission width of the resonance and is anticorrelated with the total gamma-ray energy. Such correlations could be caused by the (n,γf) reaction.[8] In the case of such a reaction,

the emission of an initial gamma ray could increase the average total gamma-ray energy emitted. Since the total gamma-ray energy could be greater, then $\bar{\nu}$ could be smaller because of less available energy. This effect would be important only on resonances where the fission width was small so that the $(n,\gamma f)$ reaction would be an appreciable fraction of the full fission width.

New data have been taken on $\bar{\nu}$ as well as the total gamma-ray energy by the presently reporting experimenters. These experiments used a fission chamber to detect fission events, fast-neutron detectors to detect the fission neutrons, and "total energy detectors"[9] to detect the fission gamma rays. No significant difference was observed in the $\bar{\nu}$ data from that previously reported.[5] Thus these results are discrepant with the new data[7] which shows an appreciably lower $\bar{\nu}$ for resonances with narrow fission widths. Concerning the total gamma-ray energy, there were a few cases where resonances with a small fission width had higher than average total prompt gamma-ray energy. The correlation is not as strong as that previously reported.[7]

Therefore, our data do not corroborate a strong correlation of $\bar{\nu}$ with the fission width of the resonances. There does seem to be a weak correlation of total gamma-ray energy with fission width as has been proposed.[7]

[1]Paper presented at American Nuclear Society, June 10-15, 1973; published in Trans. Am. Nucl. Soc. 16, 315 (1973).

[2]Instrumentation and Controls Division.

[3]S. Weinstein, R. Reed, and R. C. Block, "Proceedings of the Symposium on Physics and Chemistry of Fission," IAEA, Vienna, p. 477, 1969.

[4]Yu. V. Ryabov *et al.*, "Relative Measurements of $\bar{\nu}$ in Resonance Neutron-Induced Fission of ^{235}U and ^{239}Pu," Neutron Physics Laboratory, Joint Institute of Nuclear Research, Dubna, Report P3-5297, 1970.

[5]L. W. Weston and J. H. Todd, "Proceedings of the Third Conference on Neutron Cross Sections and Technology," CONF-710301, vol. 2, p. 861, 1971.

[6]R. W. Hockenbury, R. C. Block, and R. Reed, Rensselaer Polytechnic Institute, private communication, 1973.

[7]D. Shackleton *et al.*, "Prompt Neutron and Gamma-Ray Yields in Fission Induced in ^{239}Pu by Resonance Neutrons: Existence of the $(n,\gamma f)$ Reaction," submitted to Phys. Letters, and private communications.

[8]J. E. Lynn, "The Theory of Neutron Resonance Reactions," Clarendon Press, Oxford, p. 432, 1968.

[9]R. L. Macklin and J. H. Gibbons, Phys. Rev. 159, 1007 (1967).

6.8 MULTILEVEL EFFECTS IN THE UNRESOLVED RESONANCE REGION[1]

G. de Saussure and R. B. Perez

The calculation of the Doppler coefficient of reactivity in fast reactors requires an accurate estimate of the resonance absorption in the

unresolved energy range where actual resonance parameters are not known.[2] For the specification of the cross sections of the fissile isotopes in that region, ENDF/B-III[3] uses the single-level formalism, while an analysis of the cross sections in the resolved region indicates that a multilevel formula is necessary to represent the resonance structure.[4]

We have compared the statistical properties of the cross sections of ^{235}U and ^{239}Pu generated using ENDF/B-III with those obtained by a multilevel formulation.[5] The multilevel parameters were chosen so as to give the same average cross sections as ENDF/B-III. The comparisons were done for the S-wave part of the cross sections.

In Table 6.8.1 we give as a function of temperature the variance of the total cross sections of ^{235}U. The multilevel calculation shows a significantly larger variance, but, as expected, the variance and the difference between the two formalisms decrease with increasing Doppler broadening.

Table 6.8.1. Variance of the Total Cross Sections of ^{235}U at 500 eV as a Function of Temperature[a]

	$\langle\sigma_L^2\rangle - \langle\sigma_L\rangle^2$ (barn^2)		
Formalism	0°K	300°K	1000°K
Single Level[b]	1273±47	296±9	180±6
Multilevel[c]	1750±66	346±11	202±7

[a]In ENDF/B-III the value of Γ_f/D for ^{235}U has its maximum value at 500 eV.

[b]ENDF/B-III parameters: D = 1 eV, Γ_γ = 35 mV, Γ_n^o = .115 mV in both spin states, Γ_f = 498 mV and ν_f = 2 for J = 3; Γ_f = 249 mV and ν_f = 1 for J = 4.

[c]Equivalent multilevel parameters: Γ_γ = 24.5 mV; otherwise all parameters are as in ENDF/B-III.

The statistical properties of the cross sections may be represented in more detail by Levitt's probability tables.[6] Levitt has discussed the connection between the probability tables and reactor calculations. The probability tables obtained from cross-section ladders constructed with the two sets of parameters of Table 6.8.1 are compared in Table 6.8.2.

Table 6.8.2. Cross-Section Probability Table for ^{235}U at 500 eV[a]
(S-wave only; no Doppler broadening)

Group	σ_t Limits (barn)	P		FIS (barns)		CAP (barns)	
		Single-Level	Multilevel	Single-Level	Multilevel	Single-Level	Multilevel
1	8-10.8	0	.0006±.0003		.6±.2		.5±.2
2	10.8-14.58	.005±.001	.025±.003	2.0±.4	1.1±.1	.5±.1	.61±.06
3	14.58-19.68	.110±.005	188±.004	2.9±.1	2.11±.08	.59±.03	.68±.02
4	19.68-26.57	.288±.004	.259±.004	5.23±.07	4.91±.07	.94±.01	1.02±.01
5	26.57-35.87	.236±.003	.192±.003	9.8±.1	9.9±.1	1.75±.02	1.79±.03
6	35.87-48.43	.148±.002	.128±.002	16.2±.2	16.4±.3	3.11±.05	2.99±.05
7	48.43-65.38	.089±.001	.080±.001	24.2±.3	24.9±.4	5.32±.09	5.0±.1
8	65.38-88.26	.0534±.0008	.0497±.0009	34.1±.6	35.8±.6	9.1±.2	8.2±.2
9	88.26-119.1	.0303±.0006	.0325±.0007	46±1	48±1	15.4±.4	13.7±.3
10	119.1-160.9	.0179±.0004	.0187±.0005	59±1	65±2	26.5±.8	22.2±.7
11	160.9-217.2	.0104±.0003	.0117±.0004	74±3	80±3	43±2	38±1
12	217.2-293.2	.0057±.0002	.0065±.0002	90±4	101±4	69±3	59±3
13	293.2-395.8	.0032±.0002	.0042±.0002	100±6	115±7	112±7	97±5
14	above 395.8	.0030±.0002	.0044±.0002	104±8	129±7	220±12	211±9

[a]P = probability that the total cross section be within the limits of group; FIS = average value of the fission cross section corresponding to group; and CAP = average value of the capture cross section corresponding to group.

The comparisons shown in the tables indicate that there are small but significant differences between the statistical properties of the cross sections obtained with the multilevel formalism and those obtained with the single-level formalism. The differences may be too small, particularly when Doppler broadening is considered, to affect reactor calculations. Results qualitatively similar to those shown in the tables were obtained at 1, 5, and 10 keV as well as for ^{239}Pu.

[1]Paper presented at American Nuclear Society, June 10-15, 1973; published in Trans. Am. Nucl. Soc. 16, 328 (1973).

[2]P. Greebler and B. A. Hutchins, "Proceedings of a Seminar on Physics of Fast and Intermediate Reactors," IAEA, Vienna, Vol. 3, p. 121 (1962).

[3]T. A. Pitterle, N. C. Paik and C. Durston, "Evaluation of Integral Testing of Modifications to ENDF/B Version II Data," Westinghouse Electric Corporation, Advanced Reactor Division, WARD-4210T4-1 (1971).

[4]M. S. Moore, "Measurements on Fissile Nuclides," Experimental Neutron Resonance Spectroscopy, Academic Press, ed. J. A. Harvey (1970).

[5]C. W. Reich and M. S. Moore, Phys. Rev. 111, 929 (1958).

[6]L. B. Levitt, Nucl. Sci. Eng. 49, 450 (1972). We are indebted to J. Otter for much information and some calculations with the Probability Table Method.

6.9 THE TRANSFORMATION OF A SET OF MULTILEVEL RESONANCE PARAMETERS INTO AN EQUIVALENT SET OF SINGLE-LEVEL PSEUDOPARAMETERS AND A "SMOOTH BACKGROUND"[1]

G. de Saussure and R. B. Perez

A method is described to transform a set of multilevel resonance parameters into an equivalent set of single-level pseudoparameters and a "smooth background." The method utilizes a Kapur-Peierls expansion of the cross sections and does not necessitate "refitting" of the data. It is illustrated by an example.

[1]Abstract of paper submitted to Nuclear Science and Engineering.

6.10 TREATMENT OF LARGE PERTURBATIONS OF THE HAMILTONIAN AND THE BOUNDARY CONDITIONS OF A QUANTUM MECHANICAL SYSTEM AS AN INITIAL VALUE PROBLEM[1]

R. B. Perez and G. de Saussure

On the basis of an integrodifferential equation satisfied by the transition T-matrix, together with its associated initial conditions, we have developed a general formalism to treat large perturbations in both the Hamiltonian and the boundary conditions of a quantum mechanical system. As a result of this formalism, a set of first-order differential equations

in terms of any of the physical parameters of the system is given for the widths and poles of the collision U-matrix. In particular, an example is worked out which gives approximate expressions for these resonance parameters in the presence of intermediate structure.

The present technique is further illustrated by the conversion of a set of R-matrix resonance parameters into its equivalent set of U-matrix widths and poles, which corresponds to the passage from the R-matrix boundary conditions to the complex, momentum-dependent boundary conditions associated with the Kapur-Peierls reaction formalism. The case of large perturbations of the Hamiltonian is illustrated by the calculation of the elastic and inelastic cross sections in a strongly coupled two-channel system proposed by Tobocman and widely used as testing grounds for reaction theories.

[1]Abstract of paper to be submitted to The Physical Review.

6.11 THE OPTICAL MODEL[1]

G. R. Satchler[2] and F. G. Perey

The nuclear optical model is reviewed with emphasis on data obtained with incident neutrons and the ability of the model to aid correlation of large amounts of data on elastic scattering, absorption, and total cross sections so that predictions can be made of yet-unmeasured values. It is remarked that while the optical model works well in a qualitative sense, the quantitatively poor fits often obtained for proton as well as neutron data are suspected to be caused by poor data quality. Following a review of the theoretical basis for the optical potential itself, the paper describes recent applications of the optical model to neutron data on total cross section, elastic scattering, and inelastic scattering. Sections are also included on the isospin dependence of the potential and (p,n) reactions, spin-spin interactions, and neutron strength functions. Because of its physical significance and the variety of its applications, the concept of the nuclear optical model is felt to be "rich."

[1]Abstract of paper presented at the Conference on Nuclear Structure Study with Neutrons, Budapest, Hungary, July - August 5, 1972 (abstract written by R. W. Peelle).

[2]Physics Division.

6.12 STATUS REPORT ON THE OAK RIDGE ELECTRON LINEAR ACCELERATOR (ORELA)

J. A. Harvey,[1] T. A. Lewis,[2] F. C. Maienschein, and H. A. Todd[2]

Accelerator Operation

For the past year, ORELA has been available for research for about 5600 hours (see Table 6.12.1 for a breakdown by month). Operation continues on a 24-hr-per day, seven-days-per-week basis except for holidays. Approximately four days are scheduled for maintenance each month at times consistent with the requirements for the experimenters.

Table 6.12.1. Electron Beam Hours for Experimenters

Month	Hours
June, 1972	542.5
July	583.4
August	586.8
September	505.7
October	608.2
November	518.7
December	380.2
January, 1973	315.7
February	306.3
March	223.7
April	459.5
May	541.0
Total	5571.7

The major change in operation during the past year was made possible by the installation of a replacement gun tank in May 1972. The gun tank contains the electronics which drive the triode electron gun to produce short, high-current bursts of electrons. Due to the anode voltage of 150 kV, these electronics are operated in sulfur hexafluoride under pressure and the tank contains this insulating gas. After installation of the replacement gun tank, the repetition rate at ORELA was increased to 1000 pps, which was originally specified for the linac. Heat removal limitations in the old gun tank had not allowed extended operation above approximately 800 pps. Operation continued routinely at 1000 pps with beam power levels of 50-60 kW until February 1973 when a limitation of 800 pps was reimposed in order to reduce the consumption of spare parts and thus reduce the operating costs of the accelerator.

During operation of the linac at power levels of about 55 kW, a failure of the Be-clad, water-cooled, tantalum target occurred. This target had operated for over 5300 hr, and it may have reached the end of its useful life. The intense radioactivity induced in the target makes it very dif-

ficult to perform an analysis to determine the cause of failure, but we consider wobbling of the electron beam to be the most promising technique for reducing target failure in the future.

Electron guns have given rather short services in ORELA in the past (see Table 6.12.2). Therefore, the Isotope Development Group, including especially Joe Tracy and Ray L. Johnson, has developed over a period of time an improved electron gun. The performance of these new guns has been brilliant. They have provided currents up to a factor of 2 greater than those previously available, and the first gun of the improved type operated for 3900 hr in the linac. Its removal at that time was caused by a vacuum failure in the accelerator rather than any fault of the gun.

Table 6.12.2. Electron Gun Lifetimes

Gun Number	Beam Hours	Failure Date
Eimac 4-4	1548.3	8-1-72
ORNL No. 1	3934.9	4-27-73[a]
Eimac 8-A	551.2	5-31-73[b]

[a]Failed due to vacuum loss on accelerator.

[b]Still on accelerator.

The development and testing of improved electron guns were made possible by the use of the old gun tank as an injection-system test stand. This test stand not only allows the development of improved equipment for addition to the accelerator but permits conditioning and testing new electron guns. This operation previously required several days of accelerator time for the installation of each new gun.

Klystrons continue to operate very well as indicated in Table 6.12.3. One klystron has been operated throughout the entire history of the linac and has now accumulated more than 20000 hr. Another klystron failed last year after 12,992 hr of operation.

Table 6.12.3. Klystron Lifetimes

Klystron No.	HV Hours	
2002	1447	Original - Nov. 3, 1969[a]
2003	20829.5	Original - May, 1973[b]
2004R1	9931.7	Sept. 1971 - May, 1973[b]
2006	12921.7	Nov. 1969 - May 3, 1972[c]
2007	7850.0	Dec. 1969 - April 27, 1971[a]
2009	3106.3	Sept. 30, 1970 - April 27, 1971[a]
2010	5726.9	April 27, 1971 - April 25, 1972[a]
2011	2327.4	April 27, 1971 - Sept. 1, 1971[a]
2012	6556.5	April 25, 1972 - May, 1973[b]
2013	6396.1	April 25, 1972 - May, 1973[b]

[a]Spare.

[b]Still in accelerator.

[c]At Litton for repair.

A number of equipment changes were made during the year in order to upgrade the performance of the linac and remove demonstrated weak links. Among these was a new trigger generator which provides master signals for timing of all parts of the RF circuitry. Also replaced was the neutron monitor which was originally assembled from available components. The new system which was designed for the purpose incorporates dual channels based upon detection of neutrons in ^{235}U fission chambers. These chambers can be calibrated accurately and they are intended to have sufficient flexibility to provide an accurately reproducible indication of the neutron level both to the experimenters and to the accelerator operators. A spare accelerator section was obtained for use as a replacement when needed. Filters were added to the ORELA chilled-water system to prevent the deposition in the heat exchanger of precipitated phosphates which were used as additives in the antifreeze solution used in the system.

Data-Handling System

The Phase-I Data Acquisition System which is used for acquiring data at ORELA was brought to its full complement during the past year. This system is based on the use of small computers with a fast cycle time ($\sim$ 750 ns), each equipped with a large (0.4 to 1 x 10^6 words) disk store for experimental data. A third SEL 810B computer was installed during the year and accepted from the manufacturer in May 1973. Each of the computers can be shared by from one to four experimenters; thus the number of simultaneous experiments at ORELA is no longer limited by the availability of data-acquisition equipment.

Also during the year a controller was obtained to operate the various items of peripheral equipment and free the data-acquisition computers for exclusive attention to their primary function. Peripheral equipment includes a line printer, Calcomp plotter, card reader, magnetic tape drives, and communication links with the data-analysis system. The peripheral equipment controller was accepted from the manufacturer in October 1972.

Development of software continues for the Phase-II Data-Analysis System which consists basically of a PDP-10 computer with large mass store and a series of interactive displays and teletypes. Three of the four interactive displays are located at ORELA for use by the experimenters there. Very widespread use of the system for time-sharing is made throughout ORNL, and only a small fraction of this use occurs at ORELA. Specifically, the PDP-10 performs only minor computations in addition to serving the interactive displays, and it provides direct block transfer of substantial computations to the IBM-360, -75, or -91 computers at ORNL.

Increasingly significant use of the data-analysis system has been made by experimenters during the past year, although the development of specialized software for specific experiments is by no means completed and many additional man-years of effort will be required for this purpose. The goal for experimenters is to provide a short turnaround capability for the various steps in the analysis of experimental data. Such analysis by its nature usually requires intervention of the physicist at several

stages during the analytical process. In at least one particular application to the analysis of gamma-ray production from fast-neutron interactions (see paper 3.3 in Vol. I of this report), a clear demonstration was made of the capabilities of the data-analysis system for reducing the overall analysis time from a period of months to two to three days.

The data-analysis system has also, as expected, proven to be very useful in the evaluation of nuclear data. Such evaluation, as for the national reference data set, ENDF/B-IV, requires repeated inspections and adjustments of various sets of data which can be carried out much more efficiently with an interactive display capability than is possible with hard copy. Related advantages have been demonstrated for sensitivity studies which are used to quantitatively determine the importance of nuclear data in reactor shielding and core physics problems. Routine use of the ORELA data-analysis system is now made for this purpose in connection with the LMFBR and weapons radiation shielding programs.

[1]Physics Division.
[2]Instrumentation and Controls Division.

SECTION 7. REACTOR CORE STUDIES

7.0 INTRODUCTION

F. R. Mynatt

The work oriented toward reactor core physics consists of three areas of effort, (1) analysis and computer code development in support of radiation transport problems in reactor control and safety, particularly work for the Fast Flux Testing Facility (FFTF) Reactivity Surveillance Procedures (RSP) program, (2) a broad-based program to determine the sensitivity of reactor core design parameters to errors in the nuclear data and to provide analysis giving priorities for future cross-section measurements, and (3) analysis and code development for multidimensional core neutronics calculations, particularly the continued development of the VENTURE three-dimensional diffusion theory code but also including basic work on synthesis methods, finite element methods, fuel cycle methods, and depletion methods. In FY 1973 the majority of the core physics work was associated with task 1, the RSP program. In FY 1974 the effort will be increased and equally divided among the above three areas.

The purpose of the RSP program, previously referred to as RMASS, is to develop a technique to determine the Fast Test Reactor (FTR) reactivity status utilizing existing instrumentation methods. The program, performed in cooperation with the Instrumentation and Controls Division, involves a coupled experimental and computational effort in measurement interpretation, algorithm development, special hardware testing, and detailed reactor physics evaluations, including multigroup cross-section generation and testing.

In the area of kinetics, an analysis of various nonperturbing techniques for measuring reactivity was undertaken using the TASK one-dimensional computer code described in paper 7.1. The calculations, reported in paper 7.2, were performed using a model of the FTR-3 experiment conducted in the ZPR-IX facility at Argonne National Laboratory. A second model of the dedicated experiment in the ZPR-IX facility has been developed and calculational-experimental comparisons are currently being undertaken. The purpose of the latter is to demonstrate the use of noise analysis in inferring reactivity in subcritical systems. A model based on the FTR is currently under development.

The largest proportion of work was in the area of reactor static core calculations. The transport codes ANISN, DOT III, DOT III W, and the multi-group cross-section generation module, XSDRN, of the AMPX system were used for this purpose. Comparisons of eigenvalues and detector efficiencies were made with ANISN using the various multigroup cross-section sets currently being used in the FFTF design (paper 7.3). These comparisons indicated the effect of diffusion/transport calculations, as well as group structure and control configuration, on the ex-core monitoring system. Two-dimensional R-θ, R-Z, and hexagonal models have been developed and similar comparisons are being made in order to determine the geometric modeling effect on the ability to predict subcriticality.

Static core calculations using X-Y models in DOT III were performed on a model of the dedicated critical experiment in order to pre-determine the detector efficiencies at various positions in the core at various degrees of subcriticality and for several detector types. This effort will continue throughout the experiment.

A 30-group, ENDF III transport multigroup cross-section library was created using XSDRN for analysis of the dedicated experiment, and a similar library was created for the FTR. Results using these will be compared to other results based on pre-ENDF III sets.

Kinetics parameters for use in interpreting rod drop and noise experiments made in the dedicated critical experiment were calculated using the APC II synthesis code and COMPOZ perturbation code using techniques perfected at SEFOR (paper 7.4).

In the area of core physics sensitivity analysis, the sensitivity techni developed in the DNA-funded weapons radiation shielding program (see Section 4) are being extended for use in studying the effect of cross-section data uncertainties on important core physics parameters such as breeding ratio, multiplication factor, control rod worth, sodium void coefficient, etc. Work to date has consisted primarily of studies of the various mathematical formulations and subsequent numerical problems in determining the sensitivity matrix coefficients for core physics problems.

In the area of multidimensional core neutrons, attention is focused on the requirements for two- and three-dimensional analyses which significantly exceed the capability of present codes and computers. The VENTURE code, which is under development, will offer three-dimensional finite difference diffusion theory capability with flexible dimension programming and several modes of operation to accommodate the wide range of fast memory-peripheral storage combinations encountered with different computers and problems. Experimental computer codes are being developed to test the capabilities of a two-dimensional finite element method based on the self-adjoint form of the transport equation, a three-dimensional synthesis method for statics calculations, and improved time-dependent methods for kinetics calculations.

GFF

7.1 TASK - A GENERALIZED ONE-DIMENSIONAL TRANSPORT AND DIFFUSION KINETICS CODE[1]

A. R. Buhl, H. L. Dodds, Jr., J. C. Robinson,[2]
and R. A. Lillie[2]

The computer code TASK, written in FORTRAN-IV and using flexible dimensioning, solves the one-dimensional multigroup form of the reactor kinetics equations using either transport or diffusion theory and allowing an arbitrary number of delayed neutron groups. TASK can also be used to solve standard statics problems efficiently, such as eigenvalue problems, distributed source problems, and boundary source problems. Convergence

problems associated with sources in highly multiplicative media are circumvented and such problems are readily calculable.

TASK employs a combination scattering and transfer matrix method in order to eliminate certain difficulties which arise in classical finite difference approximations. As such, within-group (inner) iterations are eliminated and solution convergence is independent of spatial mesh size. The time variable is removed by Laplace transformation. (A later version will permit direct time solutions.) The code can be run either in an outer iteration mode or in closed (non-iterative) form. The running mode is dictated by the number of groups times the number of angles consistent with available storage.

TASK is designed for computers in the IBM-360 series; however, a preliminary version is operational on a CDC-6600 and minimal programming will be required to extend the code to other machines. A typical 13-region 5-group S_4 fast reactor statics problem requires approximately 1/2 min on the IBM-360/91, whereas the entire kinetic response can be computed in 8 to 10 min. A 16-group S_{16} static 125-cm Fe slab shielding problem requires about 4 min computation time.

[1]Computer code abstract; see Nucl. Sci. Eng. 49, 525 (1972); see also ORNL-TM-3811, "A User's Manual for TASK, A Generalized One-Dimensional Transport and Diffusion Kinetics Code," by A. R. Buhl et al. (December 1972).

[2]The University of Tennessee, Knoxville, Tennessee.

7.2 INTERCOMPARISON OF NONPERTURBING TECHNIQUES FOR INFERRING THE REACTIVITY OF FAST REACTORS[1]

A. R. Buhl, J. C. Robinson,[2] and E. T. Tomlinson[2]

Numerical experiments were performed to evaluate the applicability of nonperturbing techniques for inferring the reactivity of fast reactors. Almost all such techniques contain the tacit assumption that the flux throughout the system is described by the fundamental mode and that higher model contamination is negligible. We present results for four reactive states of a typical 1000-liter core LMFBR (critical, -1$, -7$, and -30$) which illustrate the range of applicability of the point model assumption with first-order corrections. We also point out the relative practicality of several measurement techniques.

[1]Abstract of paper submitted for publication in Nuclear Technology.

[2]The University of Tennessee, Knoxville, Tennessee.

7.3 ONE-DIMENSIONAL CALCULATIONS IN SUPPORT OF THE REACTIVITY SURVEILLANCE PROCEDURES FOR THE FAST TEST REACTOR[1]

G. F. Flanagan, D. B. Simpson,[2] and A. R. Buhl

This report summarizes the one-dimensional reactor physics models and cross-section evaluations as they pertain to the Reactivity Surveillance Procedures (RSP) Program of the Fast Flux Test Facility. It also includes a description of the techniques used to generate multigroup transport-diffusion cross sections for use in future fast reactor calculations. A study was made to examine the adequacy of using diffusion theory approximations for calculating reactor fluxes which are used in estimating neutron detector efficiencies.

Results indicate that in one dimension, the combined S_2 "diffusion" option in ANISN, along with a P_1 expansion of the cross section, gives fluxes and reaction rates which are comparable to those calculated using S_8P_3 transport theory. However, different cross-section sets used in the same model gave widely varying results, thus indicating the need for judicious selection of cross-section sets for use in the RSP Programs.

[1]Abstract of ORNL-TM-4014 (April 1973).
[2]The University of Tennessee, Knoxville, Tennessee.

7.4 CALCULATED KINETICS PARAMETERS FOR THE SOUTHWESTERN EXPERIMENTAL FAST OXIDE REACTOR ASSEMBLIES I-P, II-A, AND II-C[1]

W. A. Rhoades

The effective delayed-neutron table detailing the production of neutrons in each delay group from each fissile nuclide is calculated, together with the prompt-neutron generation time. Three SEFOR assemblies are considered, and a reference assembly is calculated using both P_0S_2 and P_3S_6 transport calculations. The generation time is sensitive to the reflector position, as is the delayed-neutron contribution of ^{238}U. The ^{239}Pu contribution was essentially invariant. The ^{235}U and ^{240}Pu contributions show some variation, but their contributions are so small that their variations are not important. A comparison with experimental data shows fair agreement.

[1]Abstract of ORNL-TM-4244 (May 1973).

7.5 VERIFICATION OF A NEW METHOD FOR CALCULATING AND MEASURING GENERATION TIME IN A SUBCRITICAL FAST REACTOR[1]

A. R. Buhl and J. C. Robinson[2]

We have verified a new method for calculating and measuring the generation time (Λ) in a subcritical fast reactor using a recently developed transfer and scattering kinetics scheme (TASK). The method is an extrapolation of a four-node fluctuations theory in which the lifetime in a thermal reactor was shown to be equal to the slope of the tangent of the phase angle from the power spectra between a high-energy-sensitive and low-energy-sensitive detector. The TASK method directly computes the prompt die-away time constant and the Λ based on the tangent method. (Present experimental techniques do not provide a direct measure of Λ for subcritical states.)

To substantiate our TASK calculations, we compared Λ with the experimental value at critical and computed Λ using the standard lambda (λ) mode and omega (ω) mode definitions for critical and for three subcritical states of the Fast Test Reactor.

[1]Abstract of ORNL-TM-3941 (September 1972).
[2]The University of Tennessee, Knoxville, Tennessee.

7.6 THE STATUS OF SUBCRITICAL REACTIVITY DETERMINATION FOR LMFBRS[1]

A. R. Buhl, N. J. Ackermann, Jr.,[2] J. C. Robinson[3]

A number of techniques have been investigated for determining the reactivity of subcritical fast reactors. Our purpose is to review several of these techniques and give our evaluation of the status of subcritical reactivity determination for LMFBR's.

Reactivity determination is important for both the design and the successful operation of LMFBR's. Models used to establish design parameters are verified in part by reactivity measurements on fast critical assemblies. Conversely, the safe and efficient operation of an LMFBR requires reliable subcriticality monitoring coupled with administrative control during shutdown and refueling operations. Reactivity determination will also be useful during initial startup for verification of certain parameters.

The objectives of these two areas of reactivity determination are somewhat different. Precision and accuracy are paramount in reactivity measurements on critical assemblies so that design parameters can be established within acceptable limits. Measurements are made in an LMFBR to verify certain design parameters and to insure safe and efficient plant operation. Of course, precise and accurate measurements are desired; however, a number of engineering constraints exist in LMFBR's which do not hamper measurements in critical assemblies. The most serious constraints

are those imposed on the neutron detection system and other measurement devices by the high temperature, gamma and electronic noise environment of an LMFBR.

A number of reactivity measurement techniques have been evaluated for application in fast critical assemblies and operating LMFBR's. The list in Table 7.6.1 is not all inclusive but rather is intended to be representative of available techniques. The list of advantages and disadvantages is also limited. The major difficulty with all techniques is that the observable quantity is never reactivity but rather a detector response (either static or time dependent) at effectively a point in the system which is then used to infer a global reactivity. The techniques in Table 7.6.1 which have been tested recently are noted and referenced. The conclusions from this evaluation are:

1. Far Shutdown. Only the modified source multiplication (MSM) technique will adequately cover the far shutdown ranges of either fast assemblies or operating LMFBR's. The MSM must be calibrated near critical, using one of the available kinetics techniques.

2. Critical Assemblies. Most of the kinetics techniques are suitable for calibrating the MSM and making measurements in the near-critical range. Some of the better techniques are inverse kinetics, break frequency noise analysis, and polarity spectral coherence.

3. Operating LMFBR's. Few kinetics techniques are suitable for calibrating the MSM or making near-critical measurements in a hostile LMFBR environment. Inverse kinetics using a ^{235}U fission counter appears the likely choice, although an asymptotic period measurement could also be considered. More sensitive detectors in suitable locations would allow the use of other techniques during initial startup (assuming a low-gamma environment).

[1]Paper presented at American Nuclear Society Meeting, June 10-15, 1973; published in Trans. Am. Nucl. Soc. 16, 289 (1973).
[2]Instrumentation and Controls Division.
[3]The University of Tennessee, Knoxville, Tennessee.

Table 7.6.1. Techniques for Inferring Subcriticality in Fast Reactors

Technique	Recent Evaluations	Advantages	Disadvantages
Amplitude Ratio	ZPR-9[1]	Not sensitive to changes in β/Λ.	Requires a calibration at critical; systematic dependence on detection efficiency; moderately difficult to implement; requires that the source strength remains constant.
Asymmetric Source Method	ZPR-9[2]	High information density.	Requires that a source with intensity greater than the inherent source be located within or near the reactor core; requires difficult calculations of asymmetric flux distributions; exact shutdown configurations must be known well in advance of application of ASM.
Break Frequency Noise Analysis	ZPR-9,[3,4] SEFOR[5,6]	Nonperturbing to reactor; no systematic dependence on detection efficiency or on sources.	Susceptible to space and energy effects; β/Λ must remain constant; difficult to implement; requires a measurement of β/Λ at critical.
Delayed Break Frequency Measurement (Noise or Rod Osc.)		Independent of changes in sources, detection efficiency, and Λ.	Very difficult to implement.
Inverse Kinetics	ZPPR,[7] ZPR-9,[8] SEFOR[5,6]	Independent of Λ changes; moderately simple to implement.	Dependent on inherent source, detection efficiency, and calculations of precise β_i fractions for each isotope; requires a large perturbation in the reactor.
Low-Intermediate Ratio		Independent of changes in source, detection efficiency, and Λ; requires no calibration.	Very difficult to implement.
Low-Zero Frequency Technique		Independent of changes in source Λ.	Requires a calibration at critical; systematic dependence on detection efficiency; moderately difficult to implement.
Neutron Source Multiplication	ZPR-9,[3,4] SEFOR[5,6]	Simple to implement; nonperturbing to reactor; not dependent on changes in Λ.	Requires a subcritical calibration near critical; systematic dependence on detection efficiency; systematic dependence on the inherent source.
Modified Source Multiplication	ZPR-9,[3,4] SEFOR[5,6]	Simple to implement; nonperturbing, not dependent for changes in Λ; detection efficiency dependence removed by calculations.	Requires a subcritical calibration; systematic dependence and changes in the inherent source.

Table 7.6.1 (Cont'd.)

Technique	Recent Evaluations	Advantages	Disadvantages
Polarity Spectral Coherence	ZPR-9[1,9]	Not sensitive to changes in β/Λ; independent of instrumentation frequency response; no systematic dependence on source strength.	Requires a calibration at critical; systematic dependence on detection efficiency; moderately difficult to implement
Pulsed Neutron Measurement	ZPR-3[10]	High information density.	Modal contamination (accented by large perturbation; requires special equipment in or near the core; β/Λ must remain constant; requires a pulsed source greater than the inherent reactor source; requires a calibration measurement.
Modified Pulsed Neutron	ZPR-3[10]	High information density; independent of changes in β/Λ.	Modal contamination (kinetic distortion); requires special equipment in or near the core; requires a large pulsed source.

[1]N. J. Ackermann, Jr., A. R. Buhl, and R. C. Kryter, "An Analytical and Experimental Evaluation of Detection Efficiency Dependence of Subcriticality Measurements by the Polarity Spectral Coherence Method," Trans. Am. Nucl. Soc. 14(1), 44 (1971).

[2]A. R. Buhl, N. J. Ackermann, Jr., and R. C. Kryter, "An Evaluation of the Asymmetric Source Technique for Determining Subcritical Reactivity in Fast Reactors," Trans. Am. Nucl. Soc. 14(1), 43 (1971).

[3]R. C. Kryter, N. J. Ackermann, Jr., and A. R. Buhl, "Measurement of Subcriticality in Large Fast Reactors by Combining Noise and Multiplication Techniques," Trans. Am. Nucl. Soc. 14(1), 42 (1971).

[4]R. C. Kryter, N. J. Ackermann, Jr., and A. R. Buhl, "Subcriticality Measurements in FTR-3: The Homogeneous Mockup of the Fast Test Reactor," ORNL-TM-3715 (1972).

[5]A. R. Buhl, N. J. Ackermann, Jr., R. C. Kryter, and J. C. Robinson, "Subcriticality Measurements in SEFOR," Trans. Am. Nucl. Soc. 15(1), 423 (1972).

[6]A. R. Buhl, N. J. Ackermann, Jr., R. C. Kryter, and J. C. Robinson, "Subcriticality Monitoring System Evaluation in SEFOR," ORNL-TM-3716 (1973).

[7]R. W. Goin et al., "Inverse Kinetics Techniques Applied to ZPPR Fast Critical Assemblies," Trans. Am. Nucl. Soc. 14(2), 794 (1971).

[8]C. E. Cohn, "Experience with Subcriticality Determination by Rod Drop in the FTR-3 Critical Experiments," Trans. Am. Nucl. Soc. 14(1), 29 (1971).

[9]R. W. Albrecht and G. M. Hess, "A Comparison of Inverse Kinetics and Polarity Spectrum Reactivity Measurements in FTR-3," Trans. Am. Nucl. Soc. 14(1), 45 (1971).

[10]W. K. Lehto, "Pulsed Neutron Measurements in ZPR-3," p. 22 in Reactor Development Program Progress Report, ANL-7518 (November 1968).

8. REACTOR SHIELDING

8.0 INTRODUCTION

C. E. Clifford and F. R. Mynatt

The objectives of the Division's Reactor Shielding Program, which has been largely supported by the AEC's Division of Reactor Research and Development (DRRD) program for the liquid metal fast breeder reactor (LMFBR) and to a lesser extent by the AEC's Space Nuclear Systems (SNS) Division, are the development of basic methods for solving radiation transport problems, the testing of these methods by comparison with experimental results, and the development of data and techniques that engineers can use with a high degree of confidence in designing shields to meet their requirements. Furthermore, the intent is to provide design techniques that are general in nature so that shields can be optimized not only with respect to weight, as required for the SNS program, but also with respect to thickness, cost, radiation heating, radiation damage, or any other requirement or constraint that may be imposed by the design engineers.

The LMFBR shielding development program has continued to increase in scope, with the highest priority effort in this program being work supporting the shielding design for the Fast Test Reactor (FTR) currently under construction. During this past year the analysis effort for FTR shielding has concentrated on neutron and secondary gamma-ray problems in the head compartment and heat exchanger vault (see Fig. 8.0.1). The important transport path for these problems begins with neutrons from fission in the core. These neutrons penetrate radially through the radial reflector and shield and induce fission in the stored fuel. The fission neutrons from the stored fuel leak into and scatter within the large radial cavity surrounding the sodium pool. Neutrons reaching the top of the cavity then penetrate upward through the radial cavity shield, the vessel support system, and the cover and on into the head compartment system, where both the neutrons and the secondary gamma rays they produce are important for contributing to the dose received by personnel. The neutrons from stored fuel fission also penetrate through the coolant pipe chaseways into the heat exchanger pipeway, where they scatter and penetrate more coolant pipe chaseways into the heat exchanger vault, where activation of secondary sodium coolant is the principal concern.

Transport analysis for these complex problems has been performed with the two-dimensional discrete ordinates code DOT and the three-dimensional Monte Carlo code MORSE. The calculations are "coupled," with output from one calculation put into a form that can be used as input in the next calculation. The first calculation is a DOT calculation of the reactor. A three-dimensional adjoint MORSE run is then made to obtain the total fission power in the stored fuel. Given the stored fuel power, a series of coupled DOT calculations with varying space and angle meshes are used to calculate the radiation field in the head compartment and heat exchanger vault. MORSE calculations coupled to forward and adjoint DOT runs are used to evaluate streaming effects in the radial cavity shield, head

ORNL-DWG 71-11788

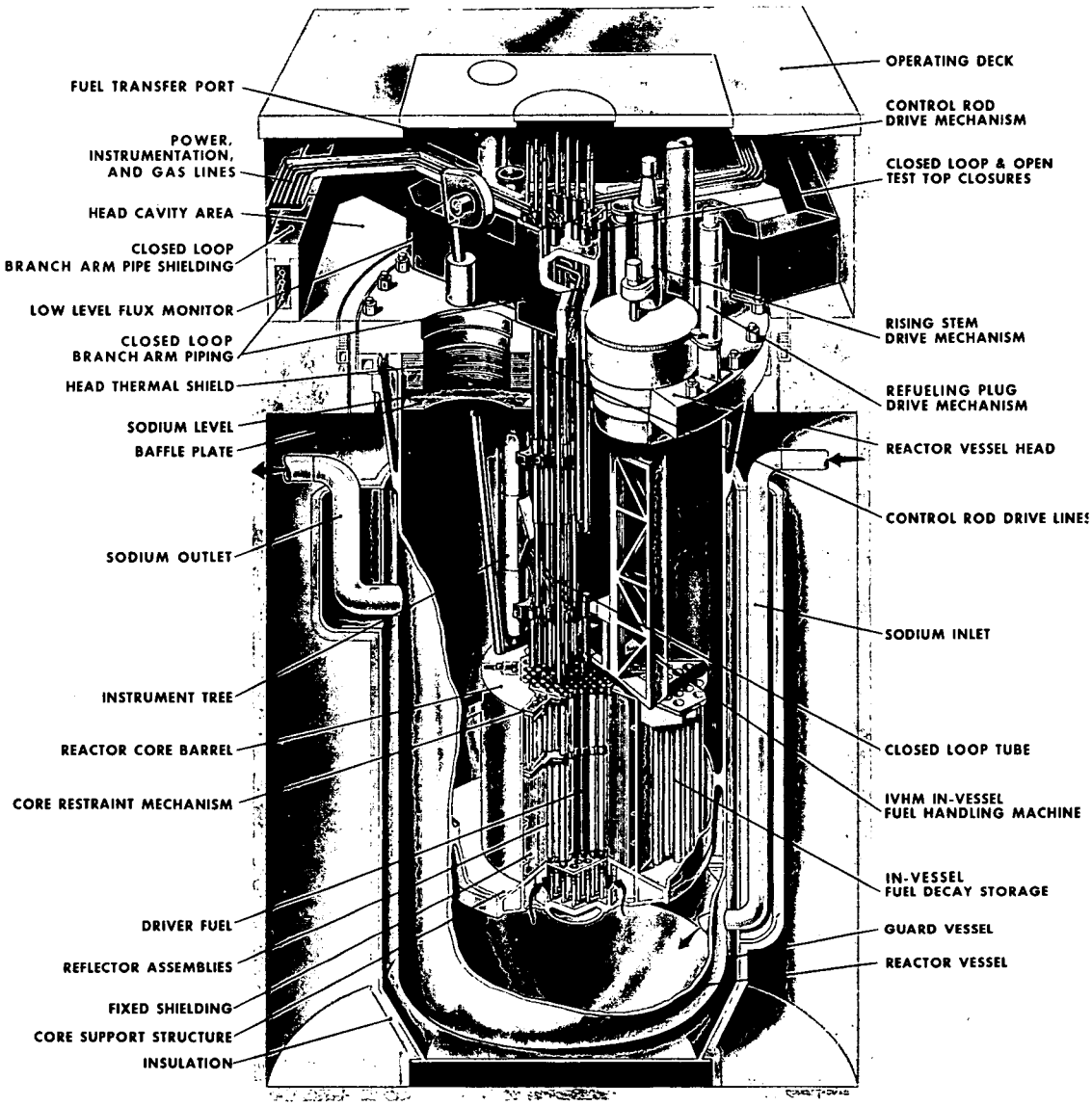

Fig. 8.0.1. The Fast Test Reactor (FTR).

compartment system, and heat exchanger pipeways. Throughout the entire procedure uncertainty analyses are performed to evaluate the effects of cross-section data, group structures, geometric models, and computational parameters such as space and angle quadrature for discrete ordinates calculations and biasing techniques for Monte Carlo calculations. Although this analytical scheme is indeed complex, automated and simplified procedures are being developed to incorporate the capability of the scheme in a more simple and computationally economical form for use by design groups.

Another major part of the LMFBR shielding program consists of integral experiments performed at the Tower Shielding Facility (TSF). The purpose of these experiments, which simulate particular problems in the LMFBR shielding, is to provide an indication of errors which may be present in the shielding calculations. Validation of the calculational part of the program is achieved by comparing experimental and calculated results, the latter being obtained from the same cross-section data sets and codes used in the shield design studies.

One series of TSF experiments was performed to verify the prediction of the gamma-ray dose rate above the FTR top head and shield configuration. In these experiments the gamma-ray spectra transmitted by thick iron shields (10 to 34 in.) was measured for two incident neutron spectra, and the effect of adding borated polyethylene to the external surface of the shield was studied. Analyses of these results, using rather crude cross-section data sets, indicated that the measured gamma-ray spectrum could be predicted within approximately a factor of two. It is anticipated that the agreement will be significantly improved by the utilization of updated coupled neutron and gamma-ray multigroup cross-section data.

Other integral experiments at the TSF have included demonstration plant shielding experiments designed by GE and Westinghouse. The radiation transported through these shields was measured utilizing both neutron and gamma-ray spectrometers. Preliminary analysis by GE of their demonstration plant axial shield mockup experiment has indicated that the radiation transport can be predicted in shields consisting of large-diameter stainless steel or boron carbide filled rods utilizing a homogeneous model to describe the shield. Measurements of the neutron fluence transmitted through a shield containing boron carbide rods 5-1/4 in. in diameter and only one row thick give no indication of neutron streaming between the rods. The space between the rods was filled with an aluminum matrix which is normally considered to be a rather poor neutron shield compared to boron carbide, and streaming was expected at least for the case of the 5-1/4-in.-diam rods. Confirmation that streaming is not a problem can greatly simplify analysis of future shield designs containing arrays of rods. This type shield is preferred in many instances to reduce the cost of very thick shields.

The Westinghouse demonstration plant experiment included in the shield mockup a UO_2 region that simulated the blanket configuration in the demonstration plant design. Blanket regions having thicknesses of 5, 10, and 15 in. were studied. The radial shield external to the blanket was mocked up utilizing layers of stainless steel, Inconel, and sodium of

the appropriate thicknesses. The full shield mockup contained a single blanket region 10 in. thick. Neutron and gamma-ray spectra were determined beyond each layer of the shield. In addition, integral measurements of neutron flux and gamma-ray dose were made utilizing uranium foils and thermoluminescent dosimeters. Preliminary analysis of these data have been completed by Westinghouse and have shown that the cross-section data set available in the Westinghouse library predicts reasonably well the measured radiation intensities behind various thicknesses of the shield.

8.1 FAST REACTOR EXPERIMENTAL AND ANALYTICAL SHIELDING MONTHLY PROGRESS REPORTS, JUNE AND JULY, 1972
189a NO. 10028, ACTIVITY NO. 40 01 61

Reports Written by:	Work Done by:	
F. R. Mynatt	R. M. Freestone, Jr.	J. J. Manning
M. L. Gritzner	M. L. Gritzner	B. J. McGregor[1]
R. E. Maerker	K. M. Henry, Jr.	J. N. Money
B. J. McGregor[1]	J. L. Hull	F. J. Muckenthaler
P. N. Stevens	J. Lewin	F. R. Mynatt
	R. E. Maerker	P. N. Stevens
		L. R. Williams

Through July, 1972, the experimental and analytical activities in the Fast Reactor Shielding Program were reported jointly in a monthly or bimonthly report. Since July, work in the two areas has been reported separately. Abstracts for the June and July, 1972, reports are as follows:

June, 1972, ORNL-TM-3928 (August 1972)

The Fast Reactor Shielding program this month consisted of detailed transport calculations for the FTR reactor cavity shielding configuration, spectrum modifier measurements for Westinghouse, final Bonner ball measurements of the TSF pipe chase experiment, and a continuation of the analysis of the pipe chase experiment.

The FTR cavity shielding calculations investigated the combined effect on the dose rate in the head compartment of a B_4C collar attached to the reactor guard vessel, a magnetite concrete shield attached to the reactor vessel support ledge, and a head compartment shield consisting of 3 in. of borated polyethylene below 1 in. of steel. The calculations consisted of a series of cylindrical-geometry DOT runs, with the output from one calculation transformed for use as input in the next. The first calculation, covering the core and part of the surrounding sodium, used 50 neutron groups, while the remaining calculations used 21 neutron groups (together with 18 gamma-ray groups). Variations in the B_4C density and full and partial magnetite concrete shields were considered. The dose rate in the head compartment increased sharply both with reduced B_4C density and reduced shielding, the lowest value calculated being 0.73 mrem/hr.

Only those Bonner ball measurements made inside the plenum in the TSF pipe chase experiment are presented here, together with the corresponding analysis performed with the DOT code. The calculations and measurements are in good agreement for the 12-in. ball, which mainly detects high-energy neutrons and in reasonable agreement for the 5- and 3-in. balls. In the case of the bare BF_3 counter, which mainly detects thermal neutrons, the calculations were too low by about 30%. The Westinghouse spectrum modifier measurements will be reported later.

July, 1972, ORNL-TM-3975 (September 1972)

The program has continued with calculations of radiation streaming through the IVHM penetration of the FTR head compartment shield; investigations of the effect of variations in iron cross-section sets, including their energy group structures, on both radial and axial FTR calculations; measurements of neutron spectra in the TSF pipe chase experiment, and an investigation of the discrepancy reported last month between the calculations and TSF measurements with the bare BF_3 counter.

In the IVHM penetration calculation, the flux penetrating to the top of the cover was calculated with DOT and transformed with the DOMINO coupling code for input in a MORSE calculation of the radiation streaming introduced by the protrusion of the IVHM into the head compartment shield. An increase of the dose rate by a factor of 100 over that for the solid shield was obtained, but these results are considered to be preliminary.

The calculations with different sets of iron cross sections show that using the latest cross sections in a 50-group structure give flux values beyond the FTR radial shield that are higher by 100% than those calculated with earlier sets. Similar calculations for the top cover yielded neutron and gamma-ray doses that are higher by 60% and 30% respectively than those calculated last month with the 21-18 group structure; thus the earlier results must be corrected.

The discrepancy reported last month between the calculated and measured responses of the bare BF_3 counter used in the TSF pipe chase experiment has been found to be due to air-scattered contributions in the measurements and to the use of thermal-neutron capture cross sections that are too high in the calculations. The TSF neutron spectral measurements made in this month are not included here, but the final Bonner ball measurements made last month in and beyond the pipe chase mockup are presented.

[1]On assignment from Australian Atomic Energy Commission.

8.2 FAST REACTOR EXPERIMENTAL SHIELDING MONTHLY PROGRESS REPORTS, AUGUST, 1972 - MARCH, 1973
189a No. 10028, ACTIVITY NO. 40 01 03 1

Reports Written by:	Work Done by:	
C. E. Clifford	R. M. Freestone, Jr.	J. J. Manning
F. J. Muckenthaler	K. M. Henry, Jr.	J. N. Money
P. N. Stevens	J. L. Hull	F. J. Muckenthaler
	J. Lewin	P. N. Stevens

August and September, 1972, ORNL-TM-4039 (November 1972)

This report presents results obtained in the Fast Reactor Experimental Shielding Program for the General Electric demonstration plant shielding experiment. Neutron spectra and fluences were measured beyond shielding configurations consisting of boron-carbide-filled stainless steel tubes 1, 2, and 5.4 in. in diameter in close-packed arrays, each array having

tubes of only one diameter. The purpose was to study streaming effects caused by the presence of a relatively ineffective neutron shield (aluminum) between the tubes, and also to provide a benchmark experiment for neutron transport in boron carbide.

Measured neutron spectra transmitted by 18 in. of stainless steel and the Westinghouse spectrum modifier consisting of 4 in. of stainless steel, 6 in. of sodium, and 1 in. of boral are also presented.

October and November 1972, ORNL-TM-4073 (January 1973)

Gamma-ray spectral data are presented for shield configurations consisting of 10- and 22-in.-thick layers of mild steel followed by 0, 2, and 4 in. of borated polyethylene. Neutron fluence determinations using a series of Bonner ball detectors are reported for all configurations, and also neutron spectra are reported for the 22-in. iron configurations. These data are part of the FTR gamma-ray benchmark experiment.

December, 1972, ORNL-TM-4127 (March 1973)

Gamma-ray spectra are presented for shield configurations consisting of a 34-in.-thick layer of mild steel followed by 0 and 2 in. of borated polyethylene. Neutron fluence determinations using a series of Bonner ball detectors are also presented for 34 in. of iron followed by 0, 2, and 4 in. of borated polyethylene. These data are part of the FTR gamma-ray benchmark experiment.

January, 1973, ORNL-TM-4170 (March 1973)

The FTR gamma-ray experiment was completed during this period, and the majority of the data for this experiment is included in this report. Development of improved techniques for the utilization of TLD dosimeters, primarily the calcium sulfate type, is described, as well as experimental results taken with the TLD's in the spectrum modifier-22 in. iron configuration tion.

February, 1973, ORNL-TM-4203 (April 1973)

The Westinghouse ARD demonstration plant side shield experiment was initiated during this period. Neutron and gamma-ray spectral measurements were completed for the spectral modifier followed by 5-, 10-, and 15-in.-thick UO_2 radial blanket configurations, as well as for several shielding configurations of sodium and stainless steel preceded by a spectral modifier and a 10-in.-thick UO_2 blanket.

March, 1973, ORNL-TM-4241 (May 1973)

The Westinghouse demonstration plant side shield experiment was continued during this period, and the General Electric radial shield study was completed. Measurements taken on the Westinghouse configurations consisted primarily of a determination of the neutron spectrum using the hydrogen counter for three radial blanket thicknesses and for the case

of a 10-in. radial blanket followed by 5 in. of stainless steel. For the GE experiments, measurements were obtained utilizing both the NE-213 neutron spectrometer and the Bonner ball detectors behind four shield configurations, which allowed a comparison of B_4C and stainless steel as alternate shield materials in a typical radial shield configuration. This report also contains a detailed description and analysis of the shielding materials utilized in both the GE and the Westinghouse experiments.

April, 1973, ORNL-TM-4252 (June 1973)

The Westinghouse demonstration plant radial shield experiment was continued during this period. Hydrogen counter measurements are reported for several of the Westinghouse configurations, including the spectrum modifier and radial blanket configurations and configurations in which essentially the full shield followed the radial blanket. Measurements are also presented on the neutrons transmitted through Inconel thicknesses of 2-1/2 and 5 in. These Inconel slabs were placed adjacent to the 10-in. radial blanket, and hydrogen counter, NE-213, and Bonner ball measurements were taken beyond the Inconel slabs to determine the transmitted neutron spectrum and fluence. The gamma-ray spectrum transmitted by the 5-in. Inconel slab was also determined. The neutron attenuation of a 5-in.-thick stainless steel slab placed beyond the Inconel was also determined using the Bonner ball detectors.

8.3 FAST REACTOR ANALYTICAL SHIELDING MONTHLY PROGRESS REPORTS, AUGUST, 1972 - FEBRUARY, 1973 189a NO. 10318, ACTIVITY NO. 40 01 03

Reports Written by:	Work Done by:	
F. R. Mynatt	R. L. Childs[2]	G. Haynes[3]
M. L. Gritzner	M. B. Emmett[2]	R. E. Maerker
R. E. Maerker	W. W. Engle, Jr.	B. J. McGregor
B. J. McGregor[1]	M. L. Gritzner	F. R. Mynatt
R. L. Childs		L. R. Williams

August and September, 1972, ORNL-TM-4040 (November 1972)

This report presents results obtained in the Fast Reactor Analytical Shielding Program from preliminary calculations of the neutron transport and activation in the FTR heat transport system; from calculations supporting the design of a spectrum modifier for a TSF experiment on secondary gamma-ray production and transport in laminated iron and polyethylene; and from MORSE calculations of the penetration of neutrons through the spectrum modifiers designed for use in the TSF experiments performed for Westinghouse and General Electric. The status of an in-progress uncertainty analysis on the reactor cavity shield (RCS) and head compartment shield (HCS) problem is also given.

October, 1972, ORNL-TM-4081 (January 1973)

The bulk of this report consists of results obtained from the analysis of the TSF measurements performed to date in the FTR iron-polyethylene secondary gamma-ray experiment. The analysis is based on DOT-III and FALSTF calculations of detector responses to neutrons and secondary gamma rays beyond 10- or 22-in. thicknesses of iron followed by 2- or 4-in. thicknesses of borated polyethylene. Calculations were also made to predict the detector responses that could be expected when the previously designed spectrum modifier is introduced in the TSF beam ahead of the iron-polyethylene configurations. Other investigations for which some results are given include (1) recalculations of the TSF FTR pipe chase streaming to determine the effect of a remeasured TSF beam source, (2) MORSE calculations of the secondary gamma rays transmitted through the Westinghouse spectrum modifier, and (3) MORSE calculations of the FTR stored-fuel power. In addition, calculations for an iron-sodium system performed with both a discrete ordinates transport method and with diffusion theory are discussed, and ORNL reports representing the first series in a CSEWG Shielding Data Testing Program are listed. Finally, the progress achieved in the uncertainty analysis of the RCS-HCS problem is described.

November and December, 1972, ORNL-TM-4164 (March 1973)

The analysis of the TSF iron-polyethylene secondary gamma-ray experiment continued with a recalculation of the earlier configurations, plus a calculation for a 34-in. iron configuration, using the latest ENDF-III iron evaluation and including the TSR-II gamma rays in the source. Results are presented for both neutrons and gamma rays. Additional calculations have also been made to improve upon and check the preliminary analysis of Phase II of the TSF FTR Pipe Chase Experiment. Neutron results are given. The effect of the ENDF-III evaluations on the earlier analyses of the sodium benchmark experiment and iron benchmark experiment was also investigated, as well as the effect of the new cross sections on calculations of the neutron transport in the FTR from the reflector to the pressure vessel along the midplane. Documentation of integral experiments for the CSEWG Data Testing Program also continued.

January and February, 1973, ORNL-TM-4231 (May 1973)

Calculations were performed with discrete ordinates and Monte Carlo methods for a conceptual FTR branch-arm-pipe shield design with a streaming path, and an update of the three-dimensional MORSE calculation of the FTR stored-fuel fission power is reported. Continuing work on analysis of the TSF FTR iron-polyethylene secondary gamma-ray experiment and DOT calculations of the large sodium experiment are reported.

[1]On assignment from Australian Atomic Energy Commission.
[2]Mathematics Division.
[3]The University of Tennessee, Knoxville, Tennessee.

8.4 SDT1 - SDT5: BROOMSTICK EXPERIMENTS TO CHECK NEUTRON TOTAL CROSS SECTIONS FOR IRON, OXYGEN, NITROGEN, SODIUM, AND STAINLESS STEEL

R. E. Maerker

In cooperation with the CSEWG Shielding Subcommittee, which is in the process of preparing documentation for certain experiments useful for testing cross sections relevant to shielding, ORNL has prepared five reports offering documentation of Tower Shielding Facility experiments that can be used to test the total cross sections on iron, oxygen, nitrogen, sodium, and stainless steel. The documentation consists of presenting the experimental data in convenient format and giving detailed specifications of the procedure by which one may perform a comparison calculation. The identification of the five reports is as follows:

SDT1: Iron, ORNL-TM-3857 Revised, ENDF-166 (September 1972).
SDT2: Oxygen, ORNL-TM-3868 Revised, ENDF-167 (September 1972).
SDT3: Nitrogen, ORNL-TM-3869 Revised, ENDF-168 (September 1972).
SDT4: Sodium, ORNL-TM-3870 Revised, ENDF-169 (September 1972).
SDT5: Stainless Steel, ORNL-TM-3871 Revised, ENDF-170 (September 1972).

For all these materials the original experiment was reported in 1968 by E. A. Straker in ORNL-TM-2242, "Experimental Evaluation of Minima in the Total Neutron Cross Sections of Several Shielding Materials."

8.5 SDT6 - SDT7: EXPERIMENTS ON SECONDARY GAMMA-RAY PRODUCTION IN IRON, STAINLESS STEEL, OXYGEN, NITROGEN AND SODIUM

R. E. Maerker

In cooperation with the CSEWG Shielding Subcommittee, which is in the process of preparing documentation for certain experiments useful for testing cross sections relevant to shielding, ORNL has prepared two reports offering documentation of Tower Shielding Facility experiments that can be used to test secondary gamma-ray production cross sections for iron, stainless steel, oxygen, nitrogen, and sodium. The documentation consists of presenting the experimental data in convenient format and giving detailed specifications of the procedure by which one may perform a comparison calculation. The first report, ORNL-TM-3957 (ENDF-176), describes an experiment in which the secondary production was due to thermal-neutron interactions in all the listed materials except oxygen. The second report, ORNL-TM-3974 (ENDF-177), describes an experiment in which the secondary production was due to fast-neutron interactions (greater than 1 MeV) in all the listed materials except nitrogen.

The original reports describing these experiments were published earlier as follows:

"Gamma-Ray Spectra Arising from Thermal-Neutron Capture in Elements Found in Soil, Concretes, and Structural Materials," ORNL-4382 (1969), by R. E. Maerker and F. J. Muckenthaler.

"Gamma-Ray Spectra Arising from Fast-Neutron Interactions in Elements Found in Soil, Concretes, and Structural Materials," ORNL-4475 (1969), by R. E. Maerker and F. J. Muckenthaler.

8.6 THE ABSOLUTE NEUTRON SPECTRUM EMERGING THROUGH A 15-1/4 in. COLLIMATOR FROM THE TSR-II REACTOR AT THE TOWER SHIELDING FACILITY[1]

R. E. Maerker and F. J. Muckenthaler

The neutron spectral intensities in a 100-group structure and the angular distribution emerging from the TSR-II reactor through the 15-1/4-in. tapered collimator at the Tower Shielding Facility are presented. These data were derived from many different measurements made at various positions along the beam centerline and may be used as free-field source terms in the calculations of experiments performed using this collimator.

[1]Abstract of ORNL-TM-4010 (December 1972).

8.7 THE ORNL BENCHMARK EXPERIMENT FOR NEUTRON TRANSPORT IN IRON AND STAINLESS STEEL[1]

R. E. Maerker and F. J. Muckenthaler

A description is presented of an experiment performed at the Tower Shielding Facility which provides verification of the accuracy of the available neutron cross sections for use in transport calculations of deep penetration of neutrons through up to 3 ft of iron and 18 in. of stainless steel. Calculations of the experiment were performed with a special version of the MORSE multigroup Monte Carlo code which uses point total cross sections. Comparison of the calculations using the new MAT 4180-MOD 1 iron cross-section set with experiment indicates that the absolute neutron leakage spectra above thermal energies arising from scattering that penetrate up to 1 ft of iron or 18 in. of stainless steel can be calculated to within about 20%, and the total neutron leakage above thermal energies penetrating up to 3 ft of iron can also be calculated to about the same accuracy.

[1]Abstract of ORNL-TM-4169 (April 1973) and of paper submitted for journal publication.

8.8 THE ORNL BENCHMARK EXPERIMENT FOR NEUTRON TRANSPORT IN THICK SODIUM[1]

R. E. Maerker, F. J. Muckenthaler, and C. E. Clifford

The description of an experiment performed at the Tower Shielding Facility (TSF) is presented which provides verification of cross-section accuracy for use in transport calculations of deep penetration of neutrons through 15 ft of sodium. Results of calculations of the experiment are presented which were obtained by using the MORSE multigroup Monte Carlo code to calculate the transport based on the ENDF/B-III cross-section set for sodium. Comparison of the calculations with experiment indicates that the total neutron leakage above thermal energies penetrating 15 ft of sodium can be calculated to within ∿30% and neutrons penetrating up to 10 ft of sodium to within ∿10%.

[1]Abstract of ORNL-TM-3960 (December 1972); papers on this subject were also presented at the National Topical Meeting on New Developments in Reactor Physics and Shielding, Kiamesha Lake, N. Y., September 12-15, 1972 (see USAEC CONF-720901, p. 418) and at Fourth International Conference on Reactor Shielding, Paris. France, October 9-13, 1972; paper has also been submitted for journal publication.

8.9 ORNL TSF PIPE CHASE NEUTRON STREAMING EXPERIMENT - PHASE ONE[1]

B. J. McGregor,[2] F. R. Mynatt,
F. J. Muckenthaler, and C. E. Clifford

Measurements were made at the Tower Shielding Facility of the transmitted neutron intensities behind three configurations of a pipe chase mockup oriented at an angle of 60 deg from the axis of a neutron beam. The three configurations considered included (1) an empty pipe chase, (2) the pipe chase containing a 16-in.-diam sodium-filled pipe, and (3) the sodium-filled pipe surrounded by insulation. Experimental results obtained included traverses with the Bonner balls just beyond the pipe exit and along the axis of the empty pipe chase configuration. The Benjamin spectrometer measurements were made at three positions 2 ft beyond the pipe chase.

A discrete ordinates transport code (DOT III) was used to calculate neutron transport through the duct configurations using a 50-group cross-section library presently being used at ORNL for FFTF shielding analysis. Good agreement between the measurements and calculations was obtained for all three configurations except for the detectors that were sensitive to the lower neutron energies, where the calculations are lower than experiment. These differences apparently indicate that a lower energy cutoff is required for the group structure. The calculated neutron energy spectrum is in good agreement with the measured spectrum covering an energy range from 50 keV to 1.5 MeV.

[1]Abstract of ORNL-TM-4176 (April 1973); paper on this subject also presented at National Topical Meeting on New Developments in Reactor Physics and Shielding, Kiamesha Lake, N. Y., September 12-15, 1972 (see USAEC CONF-720901, p. 431).

[2]On assignment from Australian Atomic Energy Commission.

8.10 FFTF PIPE CHASE STREAMING EXPERIMENT - PHASE II[1]

B. J. McGregor[2] and F. J. Muckenthaler

The present FFTF reactor design includes sodium inlet and outlet pipes which penetrate the 4-ft-thick reactor cavity wall at a height of approximately 19 ft above the top of the core, turn in the HTS pipeway, penetrate the 33-in.-thick IHX shield wall, and enter the intermediate heat exchanger vaults. Two experiments have been designed to validate analytical methods used to predict the flux levels in the FFTF intermediate heat exchanger vaults and pipeways. The first experiment (phase 1), involving a slant angle source situation was reported previously (see paper 8.9). The phase II experiment consisted of a collimated neutron beam entering a steel-lined concrete cavity containing a mockup of the pipe penetration through the IHX shield in one wall (see Fig. 8.10.1).

Measurements at the TSF have been made with six Bonner balls and the Benjamin spectrometer both inside the cavity and beyond the pipe chase exit. The three configurations used for measurements were (1) empty pipe chase, (2) sodium-filled pipe in pipe chase, and (3) sodium-filled pipe and surrounding insulation in the pipe chase.

The DOT-III code with an R-Z geometry representation was the main method of calculation. These calculations were run in two stages. A first calculation determined the fluxes and responses in the cavity which are compared to the three experimental Bonner ball traverses and the two hydrogen counter measurements in the cavity. This calculation produced an angular flux tape at the pipe chase entrance. This was converted to a source tape over a cylindrical mesh with the pipe center as axis and was used as the source for calculations with the three configurations.

The traverse most applicable to the FFTF design is that along the pipe axis beyond the pipe chase filled with sodium and insulation. As shown in Fig. 8.10.2, the calculations are 20-40% higher than the experiment with good agreement in shape. Similar agreement was obtained for the radial traverses 2 ft beyond the pipe chase and for the other configurations.

The good agreement between calculation and experiment obtained for this and the previous experiment has improved confidence in calculations of flux levels in the FFTF heat exchangers. The disagreements, however, are somewhat larger than experimental error (10-20%). To check the geometry approximations necessary for DOT and also to provide another

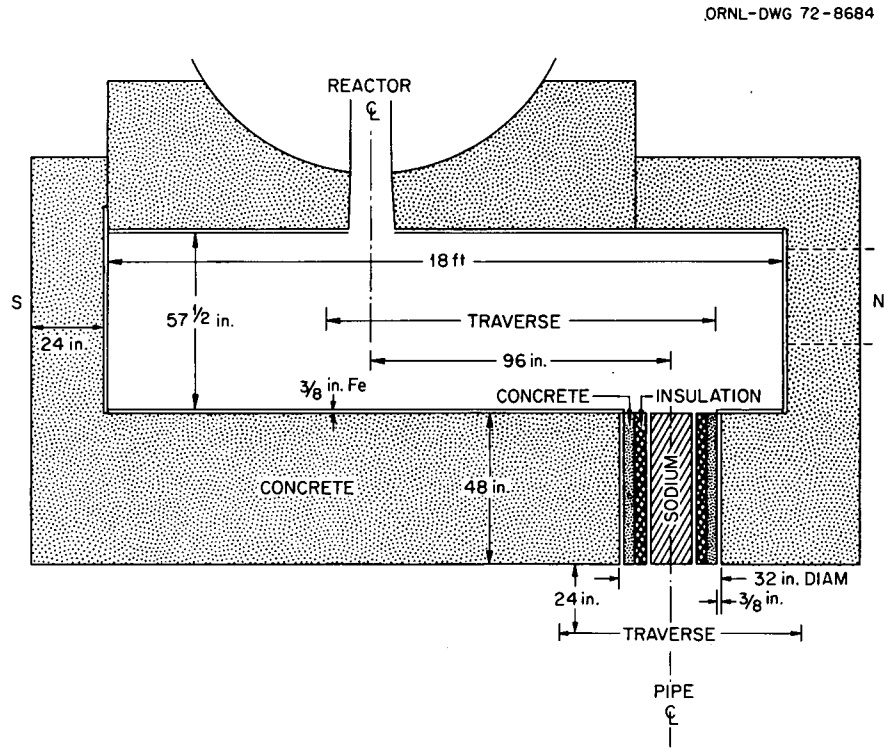

Fig. 8.10.1. Plan View of Geometry for Phase Two of TSF Pipe Chase Streaming Experiments.

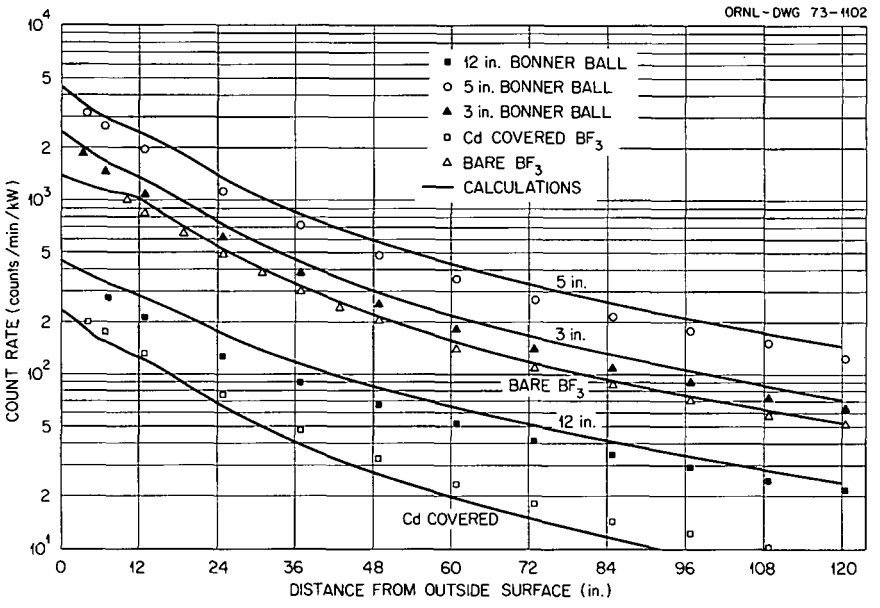

Fig. 8.10.2. Comparison of Calculation and Experiment for Pipe Axis Traverse Beyond the Assembly.

method of calculation, Monte Carlo calculations have been coupled to adjoint discrete ordinates calculations.

[1]Paper published in Trans. Am. Nucl. Soc. 16, 337 (1973); a more detailed report entitled "ORNL TSF Pipe Chase Neutron Streaming Experiment - Phase Two," will be published by B. J. McGregor, F. R. Mynatt, F. J. Muckenthaler, and C. E. Clifford as ORNL-TM-4283.

[2]On assignment from the Australian Atomic Energy Commission.

8.11 LMFBR RADIATION TRANSPORT METHODS DEVELOPMENT[1]

F. R. Mynatt, M. L. Gritzner, L. R. Williams, and C. E. Clifford

The elements of a shielding program based on a fundamental approach are discussed with a brief evaluation of the present status of the technology. A procedure is presented for utilizing the best features of Monte Carlo, discrete ordinates, and diffusion theory in coupled calculations providing good accuracy at minimum expense. As an example, results are presented from a four-step coupled two-dimensional discrete ordinates calculation for determination of the neutron and secondary gamma-ray dose rates in the FTR head compartment. An assessment of computational methods development plans is presented.

[1]Abstract of paper presented at Fourth International Conference on Reactor Shielding, Paris, France, October 9-13, 1972; also abstract of paper presented at National Topical Meeting on New Developments in in Reactor Physics and Shielding, Kiamesha Lake, New York, September 12-15, 1972 (see AEC CONF-720901, p. 480).

8.12 NEUTRON CROSS-SECTION SENSITIVITY ANALYSIS: A GENERAL APPROACH ILLUSTRATED FOR A Na-Fe SYSTEM[1,2]

D. E. Bartine,[3] E. Oblow, and F. R. Mynatt

A general approach to sensitivity studies is introduced using a quantitative definition of cross-section sensitivity. The definition offered is intended to be both practical and physically meaningful. Its advantages in comparison with other approaches are discussed and its use in analysis is illustrated for a sodium-iron transport problem. Results of the analysis include a discussion of the role of important total cross-section minima in deep penetration in sodium and iron and the importance of certain energy ranges and partial cross sections for the sodium-iron system. The predictive aspect of the approach is demonstrated in comparisons of rigorous and predicted results for small cross-section perturbations and in conclusions about the order of Legendre expansion of the scattering kernel.

[1]This work funded by Defense Nuclear Agency under Subtask PC104.

[2]Abstract of ORNL-TM-3944 (December 1972); also abstract of paper presented at National Topical Meeting on New Developments in Reactor Physics and Shielding, Kiamesha Lake, N. Y., September 12-15, 1972 (see CONF-720901, p. 512).

[3]Mathematics Division.

8.13 THE DEVELOPMENT AND APPLICATION OF A DISCRETE ORDINATES ADJOINT DIFFERENCE METHOD FOR ONE-DIMENSIONAL SHIELD WEIGHT OPTIMIZATION[1]

R. L. Childs,[2] W. W. Engle, Jr.,
J. C. Robinson,[3] and F. R. Mynatt

An improved method for the weight optimization of one-dimensional layered shields has been developed. The radiation transport problem is represented by coupled neutron-gamma-ray discrete ordinates transport calculations. In the optimization procedure, forward and adjoint calculations are performed for the initial shield design. An approximate form of the perturbed adjoint is used in the adjoint difference approach to determine the effect of shield changes, and a simple closed form optimization algorithm is used as in the ASOP code.

Three realistic shield optimization problems were solved to demonstrate the capabilities of the method. A comparison between the results obtained using this method and the ASOP code showed the agreement of the two methods to be very good and the new method to be significantly faster.

[1]Abstract of ORNL-TM-4196 (June 1973).

[2]Mathematics Division.

[3]The University of Tennessee, Knoxville, Tennessee.

8.14 A PERTURBATION METHOD FOR SHIELD WEIGHT OPTIMIZATION[1]

R. L. Childs,[2] J. C. Robinson,[3]
W. W. Engle, Jr., and F. R. Mynatt

A new method for the weight optimization of one-dimensional layered shields has been developed. The radiation transport problem is solved using the discrete ordinates computer program ANISN[4] and coupled neutron and gamma-ray cross sections. The first shield optimization technique with direct utilization of transport calculations was developed by Engle and Mynatt[5] in a computer program called ASOP.[6] In the ASOP program, each boundary position in the shield is moved twice and a separate transport calculation performed for each configuration to determine the variation of dose with boundary location for use in an optimization algorithm. Changes in dose caused by a perturbation can also be calculated using the relationship[7]

$$\Delta D = \iiint \Phi_p^+(\bar{r},E,\bar{\Omega}) \left[\iint \delta\Sigma_s(\bar{r},E'\to E,\bar{\Omega}'\to\bar{\Omega})\ \Phi_u(\bar{r},E',\bar{\Omega}')\ dE'\ d\bar{\Omega}' - \delta\Sigma_t(\bar{r},E)\ \Phi_u(\bar{r},E,\bar{\Omega}) \right] dE\ d\bar{\Omega}\ d\bar{r} \ .$$

A computer program named SHAPE is being developed which is very similar to ASOP except that the required change in dose information is obtained from the above equation. The SHAPE method requires only two transport calculations, one forward and one adjoint, for each iteration while the ASOP method requires a forward calculation for the base configuration and two for each layer boundary for each iteration. The reduction in the number of transport calculations obtained by the SHAPE method saves a significant amount of computer time.

To compare results obtained by SHAPE and ASOP, the problem described in refs. 5 and 6 was solved. The problem is a four-layer tungsten-lithium hydride shield optimization calculation in spherical geometry for a hypothetical reactor. The results obtained are shown in Table 8.14.1. Additional layers were added to the shield and the calculation repeated to demonstrate that the success of the method is largely independent of the number of layers. These results are shown in Table 8.14.2.

[1]Paper presented at American Nuclear Society Meeting, Chicago, June 10-15, 1973; published in Trans. Am. Nucl. Soc. 16, 346 (1973).

[2]Mathematics Division.

[3]The University of Tennessee, Knoxville, Tennessee.

[4]W. W. Engle, Jr., "A User's Manual for ANISN, A One-Dimensional Discrete Ordinates Transport Code with Anisotropic Scattering," USAEC Report K-1693 (1967).

[5]W. W. Engle, Jr., and F. R. Mynatt, "A Shield Optimization Technique with Direct Utilization of Transport Calculations," Trans. Am. Nucl. Soc. 12, No. 2 (1969).

[6]W. W. Engle, Jr., "A User's Manual for ASOP, ANISN Shield Optimization Program," Union Carbide Corporation, Nuclear Division, CTC-INF-941 (1969).

[7]T. J. Hoffman, J. C. Robinson, and P. N. Stevens, "The Adjoint Difference Method and Its Application to Deep-Penetration Radiation Transport," Nucl. Sci. Eng. 48(2), 179-188 (1972).

Table 8.14.1. Converged Configuration for the Sample Problem

Physical Region	Type	Outer Radius (cm)	Thickness (cm)
		ASOP	
1	Core	18.89	
2	Grid	21.93	
3	Plenum	30.60	
4	Vessel	31.08	
5	W	26.29	5.21
6	LiH	55.88	19.59
7	W	62.79	6.91
8	LiH	109.01	46.22
Weight = 1.212×10^7 g			
		SHAPE	
1	Core	18.89	
2	Grid	21.93	
3	Plenum	30.60	
4	Vessel	31.08	
5	W	36.87	5.79
6	LiH	56.36	19.49
7	W	63.03	6.67
8	LiH	108.64	45.61
Weight = 1.213×10^7g			

Table 8.14.2. Optimized Shields for Sample Problem with Additional Layers

Physical Region	Type	Outer Radius (cm)	Thickness (cm)
With Additional Layers of W and LiH			
1	Core	18.89	
2	Grid	21.93	
3	Plenum	30.60	
4	Vessel	31.08	
5	W	35.23	4.15
6	LiH	45.58	10.35
7	W	50.06	4.48
8	LiH	62.28	12.22
9	W	65.50	3.22
10	LiH	106.97	41.47
Weight = 1.133×10^7 g			
With Additional Layers of B_4C, W, and LiH			
1	Core	18.89	
2	Grid	21.93	
3	Plenum	30.60	
4	Vessel	31.08	
5	B_4C	32.00	0.92
6	W	35.76	3.76
7	B_4C	36.67	0.91
8	LiH	45.39	8.72
9	B_4C	46.35	0.96
10	W	50.84	4.49
11	B_4C	51.72	0.88
12	LiH	61.64	9.91
13	B_4C	62.48	0.85
14	W	65.12	2.64
15	B_4C	65.73	0.61
16	LiH	106.97	41.24
Weight = 1.104×10^7 g			

ORNL-4902, Volume II
UC-79d Liquid Metal Fast
Breeder Reactors Physics

INTERNAL DISTRIBUTION

1-3. Central Research Library
4. ORNL — Y-12 Technical Library
Document Reference Section
5-7. Laboratory Records Department
8. Laboratory Records ORNL RC
9. L. S. Abbott
10. F. S. Alsmiller
11. R. G. Alsmiller, Jr.
12. J. D. Amburgey
13. T. W. Armstrong
14. R. H. Baldry
15. J. Barish
16. D. E. Bartine
17. H. W. Bertini
18. F. E. Bertrand
19. A. A. Brooks
20. H. P. Carter
21. K. C. Chandler
22. G. T. Chapman
23. R. L. Childs
24. J. Ching
25. H. C. Claiborne
26. C. E. Clifford
27. H. E. Comolander
28. S. N. Cramer
29. N. F. Cross
30. G. W. Cunningham
31. F. L. Culler
32. G. de Saussure
33. J. T. DeLorenzo
34. J. K. Dickens
35. E. Eichler
36. W. E. Eldridge
37. M. B. Emmett
38. W. W. Engle, Jr.
39. S. K. Fraley
40. G. F. Flanagan
41. W. E. Ford, III
42. T. B. Fowler
43. R. M. Freestone, Jr.
44. C. Y. Fu
45. T. A. Gabriel
46. N. M. Greene
47. J. Gurney
48. R. Gwin
49. R. L. Hahn
50. W. O. Harms
51. J. A. Harvey
52. G. C. Haynes
53. R. F. Hibbs
54. H. R. Hendrickson
55. K. M. Henry, Jr.
56. O. W. Hermann
57. R. J. Hinton
58. L. B. Holland
59. J. L. Hull
60. F. B. K. Kam
61. J. M. Kallfelz
62. W. E. Kinney
63. D. L. Kirby
64. J. R. Knight
65. D. C. Larson
66. N. M. Larson
67. J. Lewin
68. R. A. Lillie
69. C. T. Long
70. T. A. Love
71. J. L. Lucius
72. R. E. Maerker
73-148. F. C. Maienschein
149. J. J. Manning
150. B. F. Maskewitz
151. J. W. McConnell
152. B. L. McGill
153. B. J. McGregor
154. G. L. Morgan
155. G. W. Morrison
156. F. J. Muckenthaler
157. F. R. Mynatt
158. C. O. McNew
159. E. M. Oblow
160. J. V. Pace
161. R. W. Peelle
162. C. M. Perey
163. F. G. Perey
164. R. B. Perez
165. L. M. Petrie
166. D. L. Reed
167. L. A. Remez
168. W. A. Rhoades

169. J. C. Robinson
170. R. J. Rodgers
171. R. W. Roussin
172. R. T. Santoro
173. D. L. Selby
174. R. J. Silva
175. E. G. Silver
176. D. B. Simpson
177. M. J. Skinner
178. G. G. Slaughter
179. P. H. Stelson
180. P. N. Stevens
181. D. Sundberg.
182. J. S. Tang
183. C. L. Thompson
184. H. A. Todd
185. J. H. Todd
186. E. T. Tomlinson
187. D. B. Trauger
188. D. K. Trubey
189. S. Uchida
190. D. R. Vondy
191. J. W. White
192. D. R. Ward
193. R. M. Westfall
194. C. R. Weisbin
195. L. W. Weston
196. J. E. White
197. G. E. Whitesides
198. H. Weaver
199. A. M. Weinberg
200. L. R. Williams
201. J. B. Wright
202. R. Q. Wright
203. I. R. Williams
204. A. Zucker
205. H. Feshbach (Consultant)
206. P. F. Fox (Consultant)
207. C. R. Mehl (Consultant)
208. H. T. Motz (Consultant

EXTERNAL DISTRIBUTION

209-210. USAEC Division of Reactor Research and Development, AEC, Washington, D.C. 20545: Director
211. USAEC-RDT Senior Site Representative, Oak Ridge National Laboratory, P. O. Box X, Oak Ridge, Tn 37830
212. USAEC Oak Ridge Operations, P. O. Box E, Oak Ridge, Tn 37830: Research and Technical Support Division
213-430. For distribution as shown in TID-4500 distribution category, UC-79d, Liquid Metal Fast Breeder Reactor Physics